



Argonne National Laboratory, with facilities in the states of Illinois and Idaho, is owned by the United States government, and operated by The University of Chicago under the provisions of a contract with the Department of Energy.

**DISCLAIMER**

This report was prepared as an account of work sponsored by an agency of the United States Government. Neither the United States Government nor any agency thereof, nor any of their employees, makes any warranty, express or implied, or assumes any legal liability or responsibility for the accuracy, completeness, or usefulness of any information, apparatus, product, or process disclosed, or represents that its use would not infringe privately owned rights. Reference herein to any specific commercial product, process, or service by trade name, trademark, manufacturer, or otherwise, does not necessarily constitute or imply its endorsement, recommendation, or favoring by the United States Government or any agency thereof. The views and opinions of authors expressed herein do not necessarily state or reflect those of the United States Government or any agency thereof.

Reproduced from the best available copy.

Available to DOE and DOE contractors from the  
Office of Scientific and Technical Information

P.O. Box 62

Oak Ridge, TN 37831

Prices available from (615) 576-8401

Available to the public from the  
National Technical Information Service

U.S. Department of Commerce

5285 Port Royal Road

Springfield, VA 22161

ANL-95/3

**Studies of Acute and Chronic Radiation Injury  
at the Biological and Medical Research Division,  
Argonne National Laboratory, 1970–1992:  
The JANUS Program Survival and Pathology Data**

---

---

by D. Grahn, B.J. Wright, B.A. Carnes, F.S. Williamson, and C. Fox

Center for Mechanistic Biology and Biotechnology  
Argonne National Laboratory, 9700 South Cass Avenue, Argonne, Illinois 60439

February 1995

Work sponsored by the United States Department of Energy,  
Office of Health and Environmental Research, under Contract No. W-31-109-Eng-38

# CONTENTS

FOREWORD .....	viii
ACKNOWLEDGMENTS .....	ix
NOTATION .....	xi
ABSTRACT .....	1
<b>1 THE JANUS REACTOR AND RELATED FACILITIES .....</b>	<b>3</b>
1.1 Historical Background .....	3
1.2 The JANUS Reactor and High-Flux Exposure Facility .....	4
1.2.1 The JANUS Reactor .....	4
1.2.2 Shutters .....	4
1.2.3 Lead Shield Plates .....	5
1.2.4 Converter Plate .....	6
1.2.5 Attenuators .....	6
1.2.6 High-Flux Exposure Room .....	7
1.2.7 Animal Irradiation .....	7
1.3 Neutron Dosimetry .....	7
1.3.1 Neutron Kerma Scanning .....	9
1.3.2 Thermal-Neutron Contribution .....	11
1.3.3 Neutron Spectrometry .....	11
1.4 Gamma Irradiations .....	13
1.5 Depth-Dose Estimates .....	14
<b>2 EXPERIMENTAL PROCEDURES .....</b>	<b>16</b>
2.1 Animal Husbandry and Housing .....	16
2.1.1 Animal Source and Supply .....	16
2.1.1.1 <i>Mus musculus</i> .....	16
2.1.1.2 <i>Peromyscus leucopus</i> .....	16
2.1.2 Housing .....	17
2.1.3 Animal Husbandry .....	17
2.2 Irradiation Procedures .....	18
2.3 Post-Irradiation Follow-up Protocols .....	19
2.3.1 Death Checks .....	19
2.3.2 Pathology Protocols .....	19
2.3.2.1 Necropsy Procedure .....	19
2.3.2.2 Collection of Tissues and Preparation for Histopathology .....	20
2.3.3 Histopathology Codes .....	20
2.4 Record Keeping and Data Management .....	21
2.4.1 Data Entry .....	21
2.4.2 Specialized Data Organization .....	22

## CONTENTS (Cont.)

2.4.3	Reliability and Potential Use of the Pathology Data	23
2.4.3.1	Analysis of Concordance between the Gross and Microscopic Pathology	23
2.4.3.2	Analysis of the Discordance between the Gross and Microscopic Pathology	24
2.5	Analytical Approaches	25
3	THE JANUS PROGRAM EXPERIMENTS	28
3.1	Introduction	28
3.2	The JANUS Series	28
3.2.1	JM-2	28
3.2.2	JM-3	30
3.2.3	JM-4	30
3.2.4	JM-7	31
3.2.5	JM-8	32
3.2.6	JM-9	32
3.2.7	JM-10	32
3.2.8	JM-12	33
3.2.9	JM-13	33
3.2.10	JM-14	34
4	SUMMARY	35
4.1	Introduction	35
4.2	The Neutron/Gamma-Ray RBE	35
4.2.1	Sex	35
4.2.2	Total Dose/Dose Rate/Protraction Period/Fractionation Pattern	36
4.2.3	Dose-Response Functions	36
4.2.4	Age at Exposure	37
4.2.5	Endpoint	37
4.3	Unresolved Issues	38
4.3.1	Dose-Response Functions	38
4.3.2	Dose Rate, Fractionation and Protraction Factors	38
4.3.3	Age at and during Exposure	38
4.3.4	Neoplastic Diseases	39
4.3.5	Other Issues	39
5	REFERENCES	40

## CONTENTS (Cont.)

APPENDIX A: JANUS Death Tag and Cage Card .....	A-1
APPENDIX B: JANUS Exit and Autopsy Codes .....	B-1
APPENDIX C: Necropsy Report .....	C-1
APPENDIX D: Protocol for Necropsy .....	D-1
APPENDIX E: JANUS MACRO Dictionary .....	E-1
APPENDIX F: Procedure for Collection of Tissues for Histopathology .....	F-1
APPENDIX G: Histology Procedure .....	G-1
APPENDIX H: JANUS MICRO Dictionary .....	H-1
APPENDIX I: JANUS ORACLE Tables .....	I-1
APPENDIX J: JANUS Radiation Protocol .....	J-1
APPENDIX K: Combined Pathology Database <E>: MACRO and MICRO Glossaries .....	K-1
APPENDIX L: Combined Pathology Database <F>: MACRO and MICRO Glossaries .....	L-1
APPENDIX M: Combined Pathology Database <H>: MACRO and MICRO Glossaries .....	M-1
APPENDIX N: List of Selected JANUS Publications .....	N-1

## FIGURES

1 Cutaway View of a Model of the JANUS Reactor and the High-Flux Room .....	5
2 Cross-Sectional View of the Reactor Shutters and Exposure Face .....	6
3 Interior View of the JANUS High-Flux Room Showing Loading System of Racks Hanging along an Isodose Surface .....	8
4 Plan View of JANUS High-Flux Room Showing Isodose Contours .....	10

## FIGURES (Cont.)

5	Neutron Energy Spectra in the High-Flux Room .....	12
6	Neutron Energy Spectra in the High-Flux Room, from Williamson and Frigerio .....	13
A.1	JANUS Death Tag .....	A-3
A.2	Cage Card .....	A-3
C.1a	Necropsy Report, page 1 .....	C-3
C.1b	Necropsy Report, page 2 .....	C-4
C.1c	Necropsy Report, page 3 .....	C-5
G.1	Slide Chart of Standard Tissues Taken .....	G-4

## TABLES

1	Composition of Combined Pathology Database <E> .....	43
2	Composition of Combined Pathology Database <F> .....	44
3	Composition of Combined Pathology Database <H> .....	45
4	JANUS Program Records Summary .....	46
5	Analysis of Concordance between Gross and Microscopic Findings for the Classifications of Lethal, Lethal Plus Contributory, and All Observed Pathology .....	46
6	Analysis of Discordance between Gross and Microscopic Pathology. ....	47
7	Inventory of Death and Pathology Records for Experiment JM-2 .....	48
8	Inventory of Death and Pathology Records for Experiment JM-3 .....	49
9	Inventory of Death and Pathology Records for Experiments JM-4K and JM-4W .....	50
10	Inventory of Death and Pathology Records for Experiments JM-4L1 and JM-4L2 .....	51
11	Inventory of Death and Pathology Records for Experiment JM-7 .....	52

## TABLES

12	Inventory of Death and Pathology Records for Experiment JM-8 .....	53
13	Inventory of Death and Pathology Records for Experiment JM-9 .....	54
14	Inventory of Death and Pathology Records for Experiment JM-10 .....	55
15	Inventory of Death and Pathology Records for Experiment JM-12 .....	55
16	Inventory of Death and Pathology Records for Experiment JM-13 .....	56
17	Inventory of Death and Pathology Records for Experiment JM-14 .....	57

## FOREWORD

In May 1994, the Center for Mechanistic Biology and Biotechnology of Argonne National Laboratory (ANL) published a report, ANL-94/26, that described the studies on acute and chronic radiation injury performed at the laboratory from 1953 to 1970. The present document covers the period from 1970 to 1992 and deals specifically with the survival and pathology data accrued during the course of the JANUS program. These data are from studies that used the JANUS reactor located in Building 202 at Argonne.

What might be the most remarkable fact about the JANUS program is that it actually came to pass. While this document cannot provide the detailed history of JANUS, both as a reactor and as a program, it can be said that the reactor itself had an unusual conception, a protracted and difficult gestation, and came perilously close to being stillborn. Conception occurred in the spring of 1958, but approval for full-power operation of the reactor finally used for the studies described in this document was not given until the spring of 1970. The intervening 12 years saw repeated safety reviews and evaluations of the reactor. In 1966, significant and unusual modifications were proposed to resolve some difficult safety and usability issues. These modifications were implemented, with the result that JANUS was born again in 1970, now as a sophisticated neutron source solely dedicated to experimental radiobiology. A brief history and description of the JANUS reactor facility is presented here with enough detail so that the unusual features can be understood and appreciated; the generation of a "clean" fission-neutron flux for experimental biology is a complex challenge.

After 22 years of successful operation, increases in operating costs, the age of the facility, and changes in program priority severely restricted the need for continuing the reactor's operation. In a letter to ANL management dated November 6, 1992, the Department of Energy ordered that the JANUS reactor be shut down. Authorization to remove the fuel elements and converter plates was given in January 1993. The elements were removed in February and March 1993, and the last fuel elements were shipped to the Savannah River Facility on March 24, 1993.

## ACKNOWLEDGMENTS

In the course of a major program that existed for about a quarter of a century, many regular staff scientists, technical staff, and temporary staff participated, contributed, and moved on. The following list includes those who participated at some time between 1965 and 1994. All manner of expertise in experimental biology, pathology, physics, and statistics is represented in this cadre, and their individual and collective contributions are herewith acknowledged with great appreciation.

### Scientific staff:

E.J. Ainsworth	R.J.M. Fry	W.K. Sinclair
T.B. Borak	D. Grahn	S.P. Stearner
P.A. Brennan	D.J. Grdina	J.F. Thomson
B.A. Carnes	L.S. Lombard	S.A. Tyler
N.A. Frigerio	G.A. Sacher	F.S. Williamson

### Technical support staff:

K.H. Allen	E.G. Johnson, Jr.	J.M. Perrin
E.J.B. Christian	D.L. Jordan	A.R. Sallese
E.M. Cooke	W.T. Kickels	M.H. Sanderson
P.J. Dale	R.A. Lea	E.F. Staffeldt
R.L. Devine	C.H. Lee	J.E. Trier
B.H. Farrington	V.A. Ludeman	C. Weber
G.L. Holmblad	M. Miller	B.J. Wright
J.L. Hulesch	M.P. Nielsen	

### Temporary staff, visiting scientists, post-doctoral appointees:

M.H. Branson	W.R. Hanson	J.H. Rust
A.V. Carrano	L.B. Hubbard	B.R. Scott
R.F. Coley	I.R. Marshall	C.P. Sigdestad
D.A. Crouse	P.J. Meechan	R.M. Vigneulle
R.C. Dickerman	P. Mitacek, Jr.	T.C.H. Yang
M.L. Garriott	B. Nagy	V.V. Yang

We also acknowledge the continued support and assistance received from the Animal Facilities veterinary staff (R.J. Flynn, DVM; T.E. Fritz, DVM; C.M. Poole, DVM) and from dozens of animal care specialists. The veterinary staff supervised the production of a consistently high-quality experimental animal, the B6CF<sub>1</sub> hybrid mouse, in adequate numbers and in a timely manner. Many of the specialists proved especially skilled in the complex, computer-controlled animal loading and unloading procedures that were an essential part of the exposure process and the individual animal's experimental history.

Obviously, consistent and reliable operation of the JANUS reactor had to be maintained for the overall program to continue according to plan. Although the (former)

Division of Biological and Medical Research did not have direct responsibility for reactor operations and safety, programmatic needs were always achieved because of highly cooperative and competent operational crews.

## NOTATION

### Abbreviations

AEC	Atomic Energy Commission
ANL	Argonne National Laboratory
BIM	Biological and Medical Research Division
Co	cobalt
He	helium
HLGF	High-Level Gamma Facility
K	kerma (measured in gray [Gy])
MAS	mean after-survival
MDI	menu-driven interface
n	neutron
p	proton
RBE	relative biological effectiveness
SE	standard error
SPF	specific-pathogen-free
U	uranium

### Units

cGy	centigray
cm	centimeter
d	day
ft	foot
g	gram
h	hour
in.	inch
keV	kiloelectron volt
kW	kilowatt
kW(th)	kilowatt (thermal)
L	liter
m	meter
μm	micrometer
MeV	megaelectron volt
min	minute
mL	milliliter
mm	millimeter
N	normal
pt	pint
R	roentgen
s	second
W	watt
wk	week
yr	year

**STUDIES OF ACUTE AND CHRONIC RADIATION  
INJURY AT THE BIOLOGICAL AND MEDICAL RESEARCH  
DIVISION, ARGONNE NATIONAL LABORATORY,  
1970-1992: THE JANUS PROGRAM SURVIVAL AND  
PATHOLOGY DATA**

D. Grahn, B.J. Wright, B.A. Carnes,  
F.S. Williamson, and C. Fox

**ABSTRACT**

A research reactor for exclusive use in experimental radiobiology was designed and built at Argonne National Laboratory in the 1960s. It was located in a special addition to Building 202, which housed the Division of Biological and Medical Research. Its location assured easy access for all users to the animal facilities, and it was also near the existing gamma-irradiation facilities. The water-cooled, heterogeneous 200-kW(th) reactor, named JANUS, became the focal point for a range of radiobiological studies gathered under the rubric of "the JANUS program." The program ran from about 1969 to 1992 and included research at all levels of biological organization, from subcellular to organismic. More than a dozen moderate-to large-scale studies with the B6CF<sub>1</sub> mouse were carried out; these focused on the late effects of whole-body exposure to gamma rays or fission neutrons, in matching exposure regimes. In broad terms, these studies collected data on survival and on the pathology observed at death. A deliberate effort was made to establish the cause of death. This archive describes these late-effects studies and their general findings. The database includes exposure parameters, time of death, and the gross pathology and histopathology in codified form. A series of appendices describes all pathology procedures and codes, treatment or irradiation codes, and the manner in which the data can be accessed in the ORACLE database management system. A series of tables also presents summaries of the individual experiments in terms of radiation quality, sample sizes at entry, mean survival times by sex, and number of gross pathology and histopathology records.



## 1 THE JANUS REACTOR AND RELATED FACILITIES

### 1.1 HISTORICAL BACKGROUND

The Division of Biological and Medical Research (BIM) of the Argonne National Laboratory (ANL) initiated a program in neutron radiobiological research in the early 1950s. A fission-neutron/<sup>60</sup>Co  $\gamma$  irradiation chamber was employed in conjunction with an open thermal-neutron column initially at the ANL research reactor CP-3' and later at CP-5 (Vogel et al. 1953). Plans to increase the reactor power level at CP-5 necessitated the consideration to build a small research reactor solely for biomedical research at BIM. Atomic Energy Commission (AEC) approval to build the reactor was given in October 1958.

The original concept of JANUS was to build a small reactor with two exposure faces to be located on opposite sides of the core (thus the name JANUS, the two-faced deity in Roman mythology). One face would be for a high-level exposure room and one for low-level exposure. The two-faced concept was attractive, although the operational requirements and constraints were never thought through. Ultimately, only the high-level exposure face was needed.

The design and construction of JANUS was not untroubled, and although initial criticality was achieved in August 1964, full power (200 kW, thermal) was not permitted for safety reasons until May 1965. Serious safety issues affecting both reactor operations personnel and users then emerged. Neutron leakage around the shutter operating mechanisms and neutron-induced activation products in the walls of the exposure rooms placed severe limitations on reactor power levels and on access to the exposure rooms. Modifications of the exposure rooms and shutters and related components were going to be required if JANUS was to become a useful research facility.

On AEC orders, JANUS was shut down while the required modifications were considered. Approval was given by AEC in early 1968 for modifications that were limited to the high-level exposure side and exposure room. The proposed modifications were actually quite clever and innovative in the fields of reactor design and physics. As a result, when all was done and JANUS was recertified in 1970, the facility emerged as a unique neutron irradiation facility with an excellent fission-neutron flux in terms of the energy spectrum, extremely low levels of  $\gamma$ -ray and thermal-neutron contamination, and a comparatively homogeneous radiation field in the exposure room that would permit large numbers of small animals to be irradiated at a single dose level at one time. Dose rate was also easily controlled by varying the reactor power level. JANUS was a perfect manifestation of the old adage, "If you've got a lemon, make lemonade." In this instance, the "lemonade" was of high quality.

## 1.2 THE JANUS REACTOR AND HIGH-FLUX EXPOSURE FACILITY

Detailed descriptions of the JANUS facility have been published in several articles (Grahm et al. 1972; ICRU 1979). The description from Grahm et al. (1972) is presented here in an abbreviated form to provide a good general sense of the overall facility, dosimetry, and exposure protocols. This descriptive material (Section 1.2.1 through the next-to-last paragraph of Section 1.3.3) has been left in the grammatical present tense; it describes the operating facility as it was between 1970 and 1984.

### 1.2.1 The JANUS Reactor

JANUS is a 200-kW(th) reactor that is cooled and moderated by light water. The core can accommodate 19 fuel elements, which consist of a uranium-aluminum alloy enriched to 93% in  $^{235}\text{U}$ . The present fuel loading is approximately 2.5 kg of  $^{235}\text{U}$ . There are two opposing faces of the reactor, which are provided with graphite thermal columns and movable shields (shutters) so that thermal neutrons may enter the exposure room adjacent to each face. Converter plates containing  $^{235}\text{U}$  may be raised into position at each face so that a source of fast fission neutrons is presented to each exposure room. At the present time, the low-flux room is not being used. Low-intensity neutron irradiations are obtained in the high-flux room by reducing the reactor power level. The system operates in a stable manner between 20 W and 200 kW to provide at least a  $10^4$  range of dose rates.

Figure 1, a cutaway view of the reactor and the exposure room, reveals the relationships among the important features. Figure 2 is a cross-sectional view of the shutters and exposure face. The important aspects of the features of the exposure room are described below.

### 1.2.2 Shutters

The high-flux room shutters are 28.25 in. (71.8 cm) thick and are fabricated to give a stepped joint at closure against the shutter pedestals. The shutters and upper part of the pedestals are designed for optimum neutron shielding, using 2 in. (5.1 cm) of lead followed by borated polyethylene bricks. The gaps between the bricks are not expected to allow significant neutron leakage paths, but, should this be a problem, the shutters and pedestals both have provision for liquid filling by vacuum impregnation. The shutters are moved in or out of position within a 5-s period by means of a pneumatic drive system located on the floor level above the reactor (Figure 2).

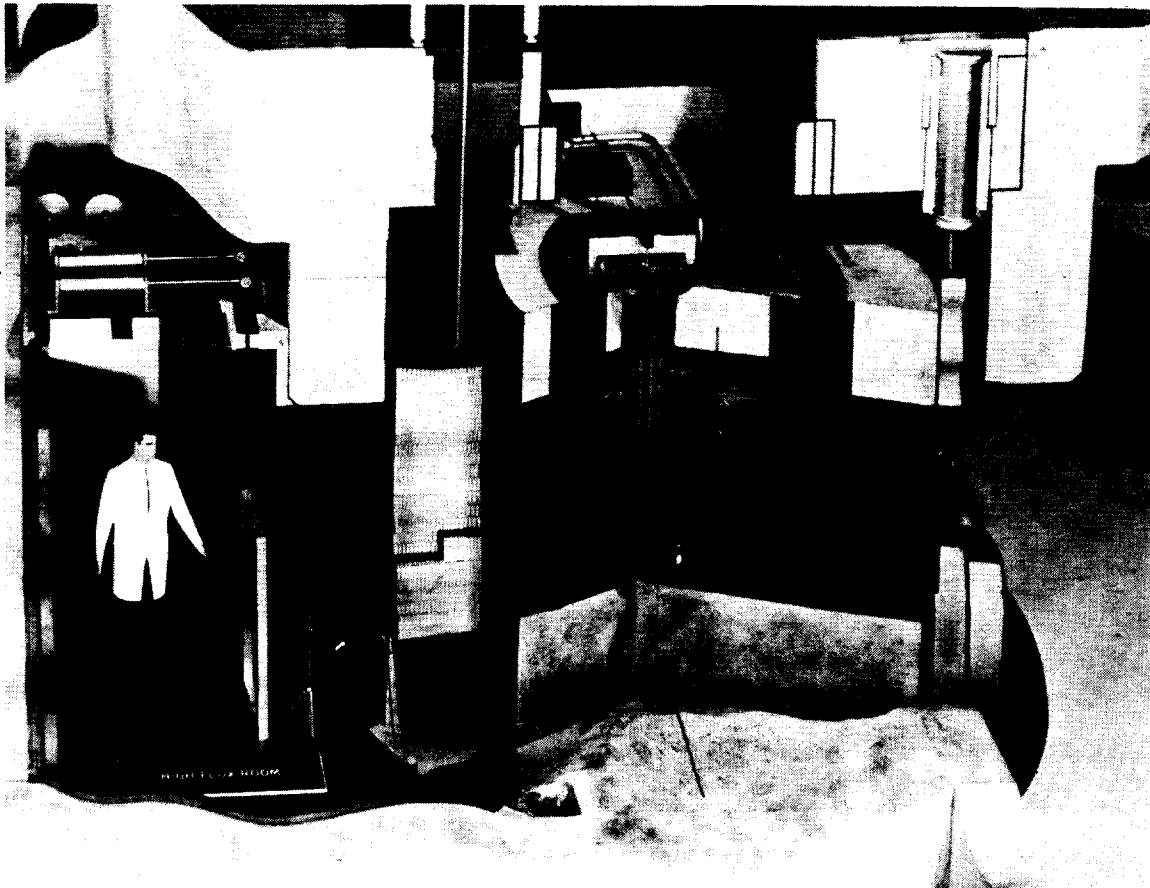


**FIGURE 1 Cutaway View of a Model of the JANUS Reactor and the High-Flux Room**

### **1.2.3 Lead Shield Plates**

To provide adequate shielding against reactor-core  $\gamma$  radiation, 9 in. (22.9 cm) of lead is interposed between the shutters and the exposure room (Figure 2). This lead is in the form of curved plates, 46 in. (116.8 cm) high, 7 in. (17.8 cm) wide, and 1 in. (2.5 cm) thick. Measurements made on a simulation of this geometry indicated that 2 in. (5.1 cm) of lead would probably reduce prompt  $\gamma$  radiation from the converter plate to an insignificant level. Because transmission through lead has a deleterious effect on the high-energy end of a fission-neutron spectrum, the 9 in. (22.9 cm) is disposed in two locations: 7 in. (17.8 cm) on the reactor side of the converter and 2 in. (5.1 cm) on the exposure room side.

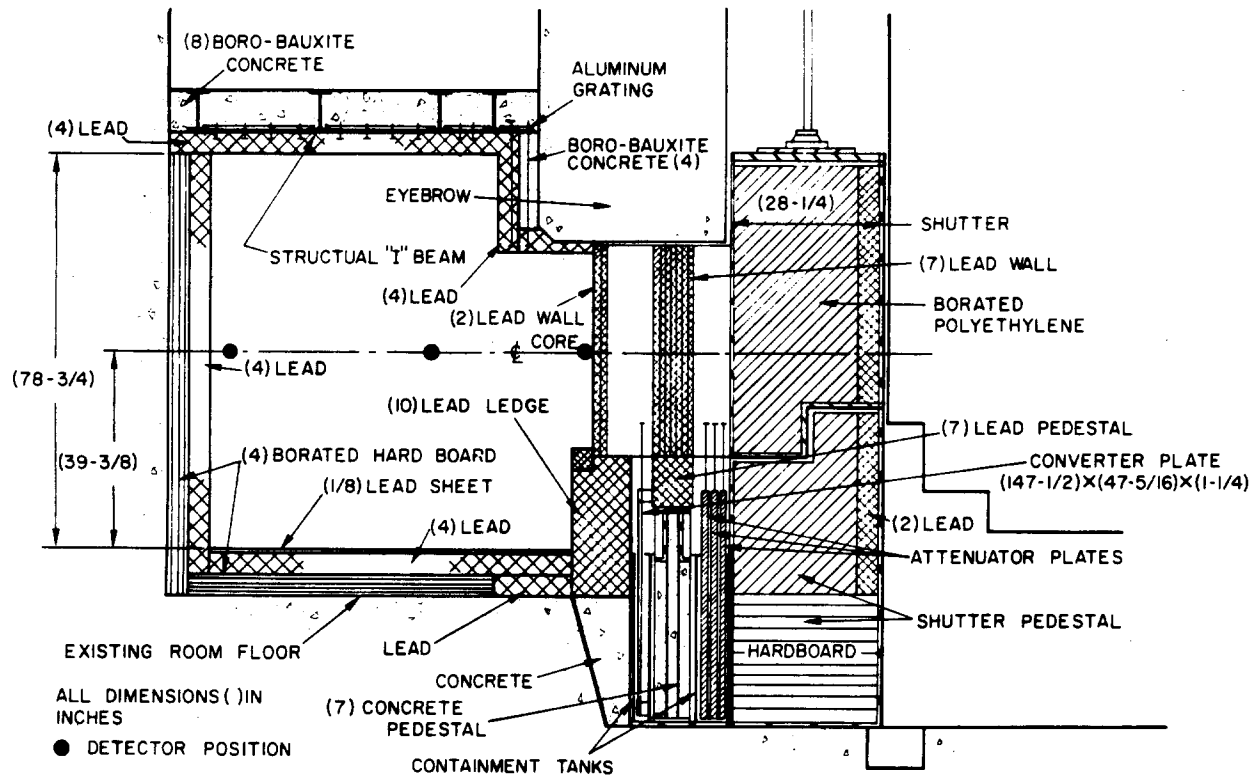


**FIGURE 2 Cross-Sectional View of the Reactor Shutters and Exposure Face (exposure room at left, reactor at right)**

### 1.2.4 Converter Plate

The converter plate contains a minimum of material that would scatter the fission neutrons and thereby degrade the spectrum. It consists of 34 foils, each 4 × 39 in. (10.2 × 99.1 cm) and 0.021 in. (0.05 cm) thick, encased in a jacket of stainless steel foil 0.007 in. (0.02 cm) thick. Each foil contains approximately 1 kg of  $^{235}\text{U}$ . The foils are clamped between curved channel sections, which form the support frame.

### 1.2.5 Attenuators

Space is provided for three attenuators between the shutters and the 7-in. (17.8-cm)-thick lead wall section, but only one attenuator is being used. This is a graded attenuator to modify the distribution of thermal-neutron flux incident on the converter plate so that the neutron isodose contour in the exposure room may be shaped as required.

### 1.2.6 High-Flux Exposure Room

The concrete walls and floor are covered by a 4-in. (10.2-cm) layer of a borated hardboard. This material is, in turn, covered by 4 in. (10.2 cm) of lead. A false ceiling consists of tiles of lead, 12 × 12 in. (30.5 × 30.5 cm) and 4 in. (10.2 cm) thick, suspended by embedded aluminum studs from an aluminum grid work supported on the lower flanges of steel I-beams. These steel flanges are coated with a neutron-absorbing paint, consisting of gadolinium oxide in a polyurethane vehicle, in order to reduce neutron activation to a minimum. The lead ceiling assembly has 8 in. (20.3 cm) of a bauxite concrete, containing boron carbide, on the upper side to reduce neutron activation in the crawl space above. The false ceiling is located so that ceiling and floor are approximately symmetrical to the center line of the reactor face; this leaves a convenient crawl space, accessible from above, for the installation of four drive systems for the converter and attenuators.

This treatment of the walls, floor, and ceiling has effectively eliminated the problem of activation  $\gamma$  radiation from the concrete. Neutrons are either reflected back into the room or thermalized by the layer of hardboard. Gamma radiation emitted by activation products that might be induced in the wall are then reduced to insignificant levels by this 4-in. (10.2-cm) lead shielding. This wall treatment has been particularly successful in reducing the thermal-neutron component of the full neutron energy spectrum.

### 1.2.7 Animal Irradiation

Mice will be irradiated without food or water, housed singly in small polyethylene containers (about 500 cm<sup>3</sup> in volume) without lids. The containers are snapped into place in a shelf module of five mice, which corresponds to one living-cage unit. The shelf prevents the mice from escaping and is perforated to provide adequate ventilation. The shelves are stacked in a loading frame of up to 12 shelves, which is hung on a framework in the exposure room (Figure 3). These frames and shelves are made from a magnesium-aluminum alloy to minimize neutron activation.

## 1.3 NEUTRON DOSIMETRY

An acetylene and argon ionization chamber pair, described by Neary and Williamson (1961), is used for kerma measurements in mixed neutron and  $\gamma$ -ray fields. Chamber constants are those calculated by Batchelor for the Harwell GLEEP (Graphite Low Energy Experimental Pile)



**FIGURE 3 Interior View of the JANUS High-Flux Room Showing Loading System of Racks Hanging along an Isodose Surface (see Figure 4)**

facility, using the variable-W model proposed by Neary et al. (1957). Chamber volumes and electrometer sensitivity are always measured by exposure in our High-Level Gamma Radiation Facility (HLGF), hence any calibration changes in that facility will have no effect on neutron/ $\gamma$ -ray relative biological effectiveness (RBE) values.

Gamma field measurements are made with an air-equivalent Victoreen Model 415 Intercomparison Standard chamber. Depth-dose measurements in all cases are made using 0.05-mL muscle-equivalent and magnesium-walled argon chambers made and contributed by the late F.R. Shonka of the Physical Sciences Laboratory, Illinois Benedictine College, Lisle, Illinois.

### 1.3.1 Neutron Kerma Scanning

A Cartesian coordinate system has been established for the exposure room. Since the reactor face is curved, the opposing wall was chosen as the base plane. The line that is normal to the reactor face at its center forms the  $z$ -axis and intersects the wall at (0,0,0). The  $y$ -axis is vertical, with the floor at  $y = -96$  cm, and the  $x$ -axis is horizontal. Thus, persons standing at the rear wall and looking at the reactor face see the face as they would a graph with vertical  $y$  and horizontal  $x$ .

Measurements made with the acetylene and argon ionization chambers at the reference location  $x = -3$ ,  $y = 0$ ,  $z = 100$  cm, with the reactor at 200 kW and without the attenuator, gave a fast-neutron kerma rate of  $23 \times 10^2$  erg/g-min with a  $\gamma$ -ray component of less than 3%. The addition of 456 phantom mice reduces the fast-neutron kerma rate by about 2%, while the  $\gamma$ -ray component maintains the same ratio.

The room was scanned at 50-cm intervals in  $x$  and  $z$  and at 25-cm intervals in  $y$  from  $-75$  to  $+75$  cm. The measurement technique was modified by adding a third electrometer connected to a Shonka tissue-equivalent ionization chamber used as a monitor. Data were obtained at 275 room locations.

These data are used to calculate the neutron and  $\gamma$ -ray kerma ratios (as a percentage of that at the reference location) for each mouse in a load frame at a specified room location and angle to the  $x$ -axis. A range of shelf positions to be used may be specified, and the average kerma ratio and individual deviations from the average can be calculated over this range of shelves.

Figure 4 shows one room layout with isodose contours corresponding to the height of mice in shelves about 100 cm above the floor.

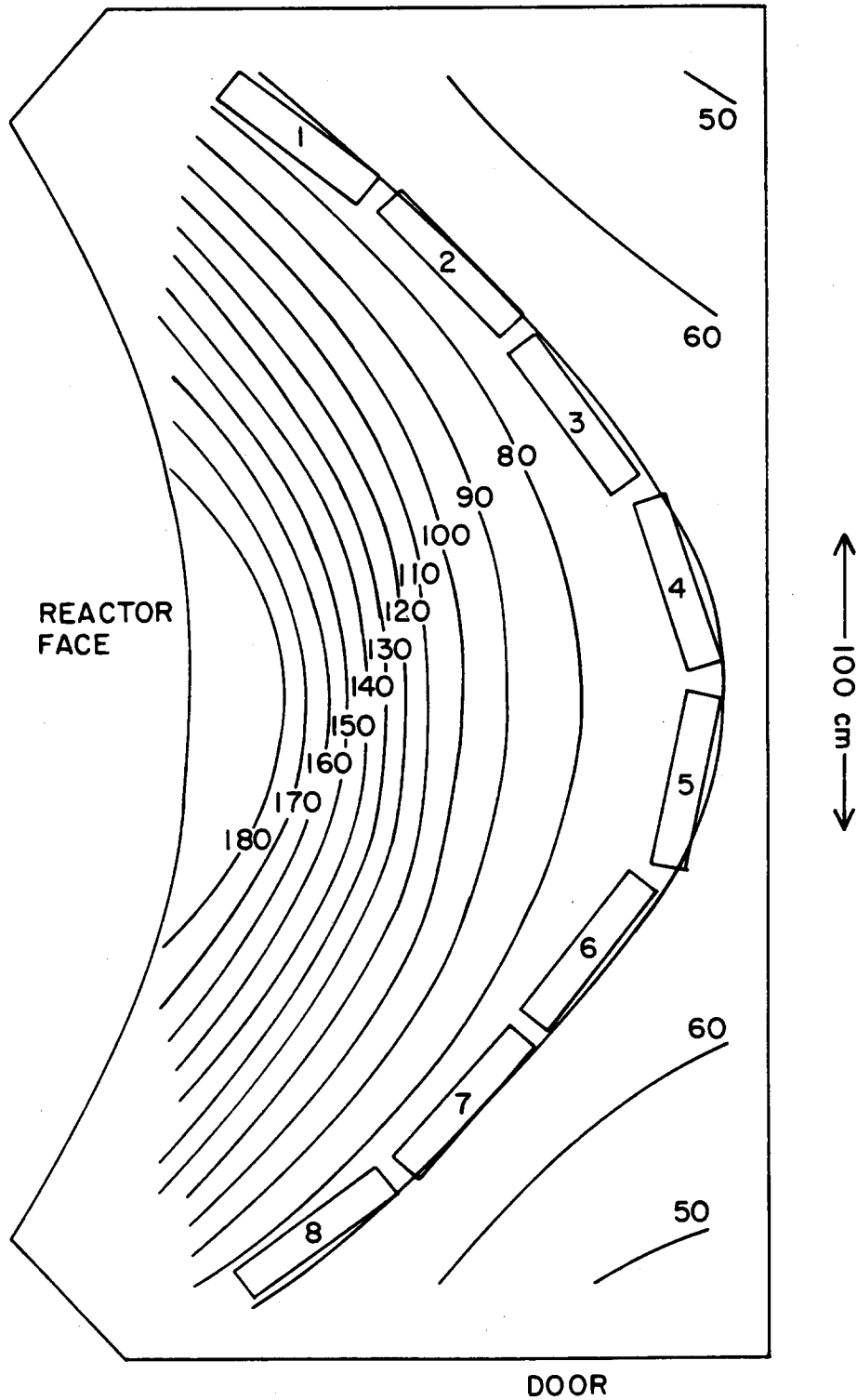


**FIGURE 4** Plan View of JANUS High-Flux Room Showing Isodose Contours. Eight load frames are indicated on one contour line (see text for details).

The contours are in percentages of kerma at the reference location with the attenuator in use. This loading layout, with use of 10 shelves per frame as seen in Figure 3, has a worst-case deviation from average of -9.7% in the top and bottom shelves of frames 1 and 8 for the individual animal locations closest to the reactor face (1% of the animal loading). The animals are placed at random in the loading frame to compensate for these deviations in dose, and the positions are monitored by the computer so that individual animal accumulated doses can be calculated.

### 1.3.2 Thermal-Neutron Contribution

Measurements with gold foils at the standard reference location, for 200 kW with no attenuator, show a thermal flux (under cadmium) of approximately  $1.72 \times 10^6$  n/cm<sup>2</sup>·s, which corresponds to a kerma rate (due to N[n, p] reactions only) of less than 0.02% of the fast-neutron kerma rate. A full load of 400 mouse phantoms approximately doubles the thermal-neutron flux and contribution. In most neutron facilities, the thermal-neutron flux is greater than that of other energy groups below 10 keV, but in the JANUS high-flux room, the walls act as thermal-neutron sinks so that this flux is depressed below the level of any other energy group. Since measurements of absorbed dose will always be made with tissue-equivalent devices, the contribution from thermal neutrons will be included.

### 1.3.3 Neutron Spectrometry

Spectra were taken at five locations in the JANUS high-flux room, identified by the  $x, y, z$  coordinates as A, in the center of the room at (0,0,100); B, at the converter lead wall (0,0,184); C, at the rear lead wall (0,0,5); D, near the unleaded room door (-129,0,50); and E, in the completely leaded corner opposite the door at (216,0,50). Effective reactor power levels were monitored over the range 100 W to 200 kW with a series of overlapping <sup>3</sup>He and <sup>235</sup>U counters, and all spectra were normalized to the reactor 200-kW level.

Spectra obtained at the central point, A, are shown in Figure 5. The proton-recoil spectrum obtained by Bennett and Yule (1972) at the same point and corrected for end and wall effects is shown for comparison. All spectra are given in absolute units and are completely independent of each other.

The arithmetic-mean neutron energy and kerma rate at the five room locations are as follows:

Room Position	Mean Energy (MeV)	Kerma Rate at 200 kW (erg/g·min)
A	0.855	$20.4 \times 10^2$
B	1.140	$51.1 \times 10^2$
C	0.716	$14.4 \times 10^2$
D	0.562	$8.9 \times 10^2$
E	0.646	$10.2 \times 10^2$

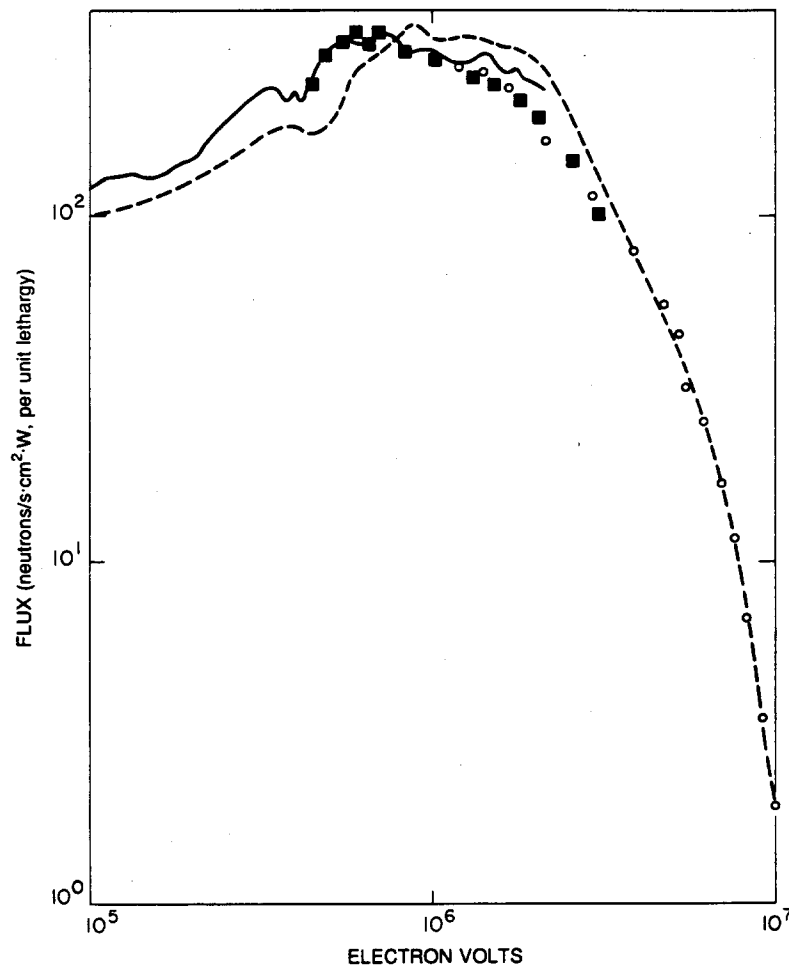


**FIGURE 5 Neutron Energy Spectra in the High-Flux Room. Solid line, proton recoil and/or  $^3\text{He}$  spectra; squares, with  $^6\text{Li}$  spectrometer; circles, with activation foils; dashed line, predicted spectrum**

The spectrum-derived kerma rates are in excellent agreement with the ionization chamber measurements.

A more complete spectrum, taken from Williamson and Frigerio (1972) and given in terms of kerma rate vs. neutron energy, is presented in Figure 6. The influence of neutron scattering on the energy spectrum can be clearly identified.

#### 1.4 GAMMA IRRADIATIONS

With few exceptions, all neutron irradiations were matched with  $\gamma$  irradiations to develop the data needed to calculate RBE values for diverse somatic and genetic endpoints. All  $\gamma$  irradiations (except for experiments JM-4L1 and JM-4L2) were done with  $^{60}\text{Co}$  sources in the HLGf located near the reactor.

The service floor of ANL Building 202, located approximately 18 ft (5.5 m) below ground level, contains both the HLGf and the JANUS high-flux exposure facility. Entrances to the two facilities are about 36 ft (10.9 m) apart and open on a common 5-ft (1.5-m) corridor. The two exposure facilities, the corridor, and the preparation and control areas share a common environment in terms of heating and ventilation, though the high-flux room itself is ventilated through a closed and monitored pathway.

The exposure room of the HLGf is  $23 \times 23 \times 18$  ft ( $6.7 \times 6.7 \times 5.5$  m), and access is through a double-L maze, entrance to which is electromechanically controlled. The walls and ceiling are 2 ft (0.6 m) thick except for the wall facing the control console, which is 4 ft (1.2 m) thick. A standard commercial unit, a Gammabeam 650 Irradiator, built and installed in April 1973 by Atomic Energy of Canada Limited, is located in the center of the room. The unit has 12 stainless steel source tubes, each containing three encapsulated  $^{60}\text{Co}$  sources, the active portion of which is approximately  $1 \times 0.5$  in. ( $2.5 \times 1.3$  cm). The unit can use a single

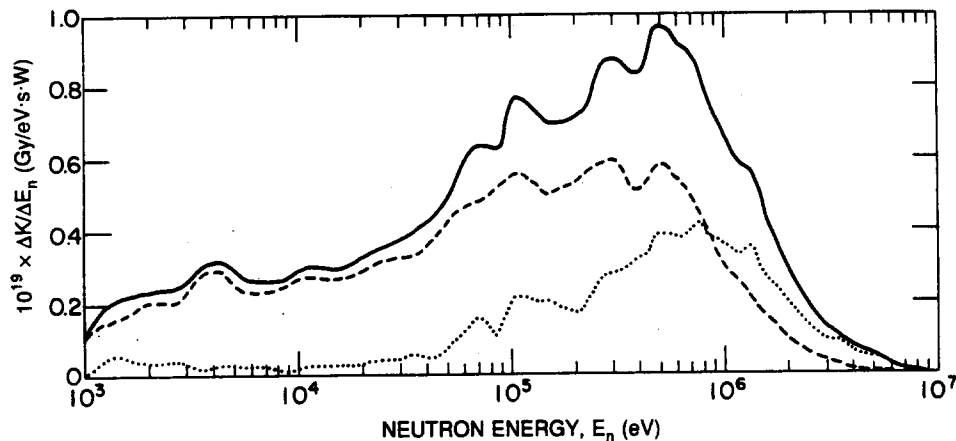


**FIGURE 6** Neutron Energy Spectra in the High-Flux Room, from Williamson and Frigerio (1972). Dotted line, at face of converter plate; dashed line, at lead wall opposite face; solid line, sum of separate spectral measurements

source tube or any number and combination of tubes up to the full 12 tubes. The many source configurations available permit exposures at a 1-m distance that range from about 20 to 30,000 R/h. Curiages (the radioactivity in curies at the sources) range between 18 and 5000. Mean source height above the floor is 68 in. (172.7 cm). The source storage cask rests on the floor and is 50 in. (127 cm) tall and 35 in. (88.9 cm) in diameter. Therefore, the exposed sources are only 18 in. (45.7 cm) above the cask.

Field dosimetry in the HLGf uses a Victoreen Model 415 chamber. As in the JANUS high-flux room, a given dose rate measured from a fixed source forms a doubly concave isodose surface or contour. The curvature is obviously more prominent in the HLGf because of the point source compared with the broad exposure face of JANUS. Within a single exposure frame hanging vertically in the contour, the worst-case deviations from the average are about -12% at 1.3 m from the source and -5.5% at 2.2 m. These deviations occur in the top and bottom shelves in the 10-shelf exposure frame (see Figure 3). For a multiple-exposure series, the deviations are averaged out by a computer-managed randomization of the location for each mouse as it is repeatedly exposed. For single exposures, the irradiation procedure avoided loading animals in the extreme locations of the frames.

The Gammabeam 650 was used for all experiments described in this report except for the first, JM-2, and for the two low-dose-rate studies, JM-4L1 and JM-4L2. The irradiations for JM-2 were carried out between March 1971 and June 1972 and used the original sources and source-handling mechanisms installed in the HLGf in 1954 and 1958. Those sources were 12-in. (30.5-cm) linear  $^{60}\text{Co}$  rods encapsulated in stainless steel and held about 48 in. (121.9 cm) above the floor (the source storage cask was in the floor). The original HLGf was constructed as part of the original Building 202 in 1950-1952, along with the low-level facility described by Grahn et al. (1994) in the pre-JANUS archive document for the 1953-1970 period. At the time, they were unique among AEC facilities, though, in retrospect, they were little more than large concrete pillboxes. The original source-handling mechanisms were designed, built, and installed by the then-existing Remote Control Engineering Division at ANL.

## 1.5 DEPTH-DOSE ESTIMATES

A critical factor in the development of data that can be used for accurate comparisons of the effects of neutrons vs.  $\gamma$  rays concerns the dose terms. Obviously, the two radiations, fission neutrons and  $^{60}\text{Co}$   $\gamma$  rays, had to be "normalized" before comparisons could be made. Normalization was achieved by making the dose term a tissue dose, specifically, the midline tissue dose for the mouse. Unfortunately, the dosimetric procedures and results have never been presented in complete form in a single report; however, much information can be gleaned from Grahn et al. (1972), Williamson and Frigerio (1972), Williamson et al. (1971, 1972, 1973), Borak and Stinchcomb (1979), and Marshall and Williamson (1985). A brief description of the results of the depth-dose studies is presented here.

A 30-g "muromorphic" mouse, having dimensions of  $5 \times 3 \times 2$  cm and made of a tissue-equivalent plastic known as Shonka A150, was used for the studies. Dr. F.R. Shonka,

of Illinois Benedictine College, developed the tissue-equivalent plastic and also constructed a pair of 0.05-mL ionization chambers to be used in the tissue-equivalent mouse. The elemental composition of the A150 plastic, in terms of percent by weight, was as follows: H = 10.25, C = 77.28, N = 3.49, O = 3.99, F = 2.43, and Ca = 2.57.

Two 0.05-mL chambers were used to measure doses at the approximate center of the phantom. One chamber was made of tissue-equivalent material; the other was of magnesium and was filled with argon. Measurements of dose were made with the phantom at five different orientations to the  $\gamma$ -ray source or to the reactor face:  $0^\circ$  (nose to the source),  $45^\circ$ ,  $90^\circ$ ,  $135^\circ$ , and  $180^\circ$  (tail to the source). Measurements were also made without the phantom. The average midline neutron dose in rads was 80% of the neutron kerma "in air." For  $\gamma$  radiation, the midline dose was 90% of the measured roentgens "in air." Specifically, for  $\gamma$  rays, the ratios were 0.96  $K/R$  and 0.934 midline tissue dose rad/ $K$  ( $0.96 \times 0.934 = 0.897$ ). The delivered doses in the JM studies were the calculated midline tissue dose values measured in rads (0.01 Gy). Details can be found in Grahn et al. (1972), Williamson and Frigerio (1972), Williamson et al. (1972), and ICRU Report 30 (1979). Because all delivered doses were midline tissue doses, dose-response coefficients in terms of response per rad of  $\gamma$  rays or neutrons can be directly applied to the estimation of RBE values or other measures of fission-neutron effectiveness when compared with responses to  $^{60}\text{Co}$   $\gamma$  rays.

## 2 EXPERIMENTAL PROCEDURES

### 2.1 ANIMAL HUSBANDRY AND HOUSING

#### 2.1.1 Animal Source and Supply

##### 2.1.1.1 *Mus musculus*

All of the JM series studies used the B6CF<sub>1</sub> mouse, the F<sub>1</sub> from the cross of C57BL/6 females with BALB/c males. The parent inbreds were originally obtained from the Jackson Laboratory, Bar Harbor, Maine, in 1953 (Grahn et al. 1994) and were maintained by full-sib matings as conventional stocks. In 1965, breeding stock from the two strains were given to the ANL animal facilities staff, under R.J. Flynn, DVM, to produce a germ-free breeding stock from which specific pathogen-free (SPF) strains could be derived for the production of large numbers of B6CF<sub>1</sub> mice for the JANUS program. The correct designations for these SPF parent strains are BALB/c ANL (ANL 66) and C57BL/6/ANL (ANL 66). The "(ANL 66)" designates the institution of origin and the year when the SPF status was obtained. The inbred strains were rederived in 1970, so some records will note B6CF<sub>1</sub>/ANL (ANL 70), others B6CF<sub>1</sub>/ANL (ANL 66). This is not a critical difference. The strain is numerically coded as 08, following from its original designation in 1954 (Grahn et al. 1994).

The SPF status was periodically checked by the animal facilities staff and by commercial laboratories. No unusual or unacceptable microbiological or virological deviations from the SPF status were noted over the years. All mice were vaccinated for ectromelia (mouse pox) before entry into an experiment.

Animals were weaned into large cages with dimensions of approximately 16 × 8 × 5 in. (40.6 × 20.3 × 12.7 cm, length by width by height), 15 or 20 to the cage. At 110 ± 5 d of age, the mice were recaged into small plastic cages of 11 × 7 × 5 in. (27.9 × 17.8 × 12.7 cm), five per cage. These cages were then randomly assigned to their ultimate experimental status and to holding rooms in the animal facilities.

##### 2.1.1.2 *Peromyscus leucopus*

In 1963, G. Sacher and E. Staffeldt trapped wild *Peromyscus leucopus* (the white-footed deer mouse) on the Argonne site and established a breeding colony in the animal facilities. Additional breeders were periodically captured in the wild. The colony was maintained by random outcross matings, and conventional caging and husbandry methods were employed. Though G. Sacher performed a number of radiobiological and gerontological studies with *P. leucopus* and other small mammals taken from the wild, *P. leucopus* was selected for use in the JANUS program for one major study (JM-10). This study compared responses to single and fractionated neutron and  $\gamma$ -ray exposures with those seen in the B6CF<sub>1</sub> subjected to the same exposure regimes. *P. leucopus* is slightly larger than the B6CF<sub>1</sub>

mouse, ranging from 20 to 45 g at about 140 d of age when they were entered into the study. Their life expectancy from birth is about 1450 d (Sacher and Hart 1978), which is about 50% greater than that of the B6CF<sub>1</sub> mouse.

### 2.1.2 Housing

A critical lesson that was learned in the early studies (Grahn et al. 1994) concerned the importance of maintaining both experimental and control animals in a common environment. In the JANUS studies, this was accomplished by keeping all mice in a common home environment or animal rooms except when actual irradiations were performed. All controls, with one exception (JM-7), were sham-irradiated in the corridor of the service floor between the HLGF and the reactor. As previously noted, all mice were housed in a clear plastic cage, five per cage. The stainless steel cage top was screened in the back half and held a water bottle and food bin in the front half. Originally, a corncob bedding was used, but it was found to carry the organism *Enterobacter cloacae*, which caused an acute intestinal syndrome. Sterilized wood chip shavings were thereafter consistently used for cage bedding.

Room management and housing assignments were made by a computer-generated procedure. Cages were located (according to experiment) in home rooms and positioned on a random basis with respect to radiation quality (including control), sex, treatment dose and exposure pattern, replication number, and cage number. The animals in every experiment were always located (housed) in two or more separate animal rooms to minimize any effects due to differential room environment.

### 2.1.3 Animal Husbandry

Routine animal care was the responsibility of the animal facilities staff and was carried out by trained and experienced animal care specialists. Periodic sampling of food, water, feces, etc. for infectious organisms was performed by the scientific staff of the animal facilities. During the period that the JANUS studies were being carried out, the ANL animal facilities were fully accredited by the American Association for the Accreditation of Laboratory Animal Care.

Cages would normally be changed weekly but more frequently if conditions required. Water bottles were changed twice weekly, and the water was acidified to  $\text{pH } 2.5 \pm 0.1$  with 0.1 N HCl. This successfully eliminated water-borne infection by *Pseudomonas aeruginosa*. Acidified water did not otherwise influence the health status of the mice. Food was always available and was normally Wayne Mouse Lab Blox. All rooms and cages were checked every day (7 d/wk).

The animal rooms were maintained at  $73 \pm 3$  °F ( $22.8 \pm 1.7$  °C) and humidity at  $50 \pm 5\%$ . Filtered and conditioned air was turned over between 10 and 15 times per hour and was exhausted into the corridors of the animal facilities. Animal holding rooms were at a positive air pressure compared with that of the hallways. There were no windows in the

animal facilities, and a 12-h light/dark cycle was maintained with electric timers; the light period was from 6 AM to 6 PM.

## 2.2 IRRADIATION PROCEDURES

Special exposure frames were used for all irradiations. These were constructed of a magnesium-aluminum alloy (to minimize neutron activation) and had dimensions of about 5 ft (1.5 m) in height by 2 ft (0.6 m) in width. They were suspended from ceiling hangers in the JANUS high-flux room (Figure 3) and from portable floor stanchions in the HLGf. A frame could hold up to 12 shelves (10 were normally used), each suspending five 1-pt (0.5-L) polyethylene cups in a row, each cup holding one mouse. Missing mice were replaced by a tissue-equivalent dummy. Because the frames occupy a vertical space in a nonlinear isodose contour, only those shelves were used for a given exposure where the deviation from mean dose would be less than 10%.

The frames were loaded by the animal care specialists, according to computer-generated loading instructions. Each frame contained mice to be located in a single dose group, although several frames could be used for each dose. Cages to be loaded were identified by the animal identification code and the cage location in the holding room. Sham-irradiated controls were handled exactly as the mice to be irradiated, but their frames were hung in the hallway outside the JANUS and HLGf rooms. After irradiation, frames were unloaded in the home rooms by the animal care specialists according to computer-generated instructions.

Long-term exposures (22 h/d) in the low-level  $\gamma$ -ray facility, used only for experiments JM-4L1 and JM-4L2, employed the same frame, basic shelf unit and 1-pt (0.5-L) cups, but the units were modified to hold a 5-oz (0.15-L) plastic water bottle and a spring-loaded vertical feeder unit behind the bottle. Wood chip litter was provided for the individual mouse in each cup. Mice remained in this housing unit for 5 d of each week of exposure, Monday morning to Saturday morning. The other 2 d were spent in the standard home cage, five mice per cage. Controls and irradiated mice were handled in the same manner, with the controls remaining in the corridor of the facility entrance maze.

We emphasize that for all of these exposure procedures, computer programs managed all operations and randomized all cage loadings per dose, sex, and radiation quality, for each replication within the specific dose contour, so that all deviations from mean delivered dose would be randomly distributed among all mice within the dose group. The computerized randomization process that managed all irradiations and housing locations is the manifestation of the policy to minimize, or even eliminate, any environmental or irradiation heterogeneity that might confound response variables or challenge the credibility of any finding.

## **2.3 POST-IRRADIATION FOLLOW-UP PROTOCOLS**

### **2.3.1 Death Checks**

Throughout the JM experimental series, mice were usually relocated within the animal facility after their irradiations were completed. This facilitated the death checks that were performed daily, 7 d/wk, including holidays. On regular work days, members of the program staff performed the checks, usually twice daily. The afternoon check would identify moribund animals that were expected to die overnight. Moribund mice were euthanized with ether. On weekends and most holidays, death checks were performed once daily by animal care specialists who were experienced in this procedure.

A dead animal was removed from the cage and placed in a disposal bag, and a JANUS death tag was stapled to the bag. A sample copy of the death tag and a copy of a cage card, from which the essential identification data were taken, are seen in Appendix A. The cage card contained all information pertaining to the identification and location of the dead mouse. The animal identification code included the radiation quality (C, control; G,  $\gamma$  ray; N, neutron); the sex (M, male; F, female); treatment group, which is usually a dose code; replication number; and cage number. This provides an eight-character alpha-numeric code for the identifying "family name." The number of animals in a cage ranged from 1 to 5. The individual animals were not preidentified. Numbering was based on which died first, second, . . . , fifth; number 1 was the first recorded and number 5 the last. This individual number gave a "first name" to each animal, and thus, the nine characters provided each animal with a unique identification. The death tag was filled out with the appropriate information from the cage card that identifies the experiment, animal identification code, date of death, etc. The date of death was entered on the cage card and the card was returned to the cage. The dead animal was either refrigerated or taken directly to the necropsy prosector. According to the condition of the animal, the prosector determined if a necropsy should be done. Ultimately, an exit code and an autopsy code were assigned to the individual identified on the death tag, and the codes were entered along with the date of autopsy and the initials of the prosector. The exit codes and autopsy codes are defined in Appendix B.

### **2.3.2 Pathology Protocols**

#### **2.3.2.1 Necropsy Procedure**

The necropsy report (Appendix C) is made up of three pages: page 1, coded MACRO observations; page 2, a carbon copy of the top of page 1 that was used to enter the MACRO data into the computer; and page 3, coded MICRO diagnoses. The first page was filled out as the necropsy was performed. The data from the JANUS death tag were transferred to the necropsy report, and the death tag number (upper right corner) became the autopsy number. As the necropsy progressed, sketches of lesions and tumors were placed on

the drawings of the mouse, observations were circled, and the tissues fixed were indicated in the appropriate boxes at the bottom of the page.

The necropsy protocol, presented in detail in Appendix D, specifies the gross characteristics to be identified or sought out for all organs and tissues by the prosector. It also describes the specific appearances of organs and tissues that are directly defined by specific gross pathology codes. The full MACRO dictionary of three-letter nontumor and four-letter tumor codes is given in Appendix E in alphabetical order. Part 6 of Appendix D discusses the criteria to be considered for establishing a probable cause of death on the basis of the gross findings. The probable cause of death was entered on the necropsy report. In addition, the presence or absence of a tumor was indicated as T or NT, and MACRO diagnoses were recorded as tumor or nontumor codes. After the necropsy was completed, the second page of the necropsy report was removed and used to enter the gross pathology into the computer MACRO records for the experiment.

### **2.3.2.2 Collection of Tissues and Preparation for Histopathology**

Tissue sampling for histopathology followed a standard procedure throughout the JM series. In some studies, selected additional tissues might have been taken for special purposes, but the procedure outlined in Appendix F can be considered the basic protocol. The procedure for fixing, staining, and mounting the tissues on slides is outlined in Appendix G. Obviously, not all tissues or organs were routinely sampled, other than those listed, and no effort was made to detect occult tumors or other lesions that were considered to be noncontributory to the animal's death. As stated in the original description of the JANUS program in 1972 (Grahm et al. 1972), the intention was always "to ascertain the cause of death to as high a degree of accuracy as practicable." We were concerned, as well, with all major contributory and noncontributory pathology. Although funding and manpower limitations forced some compromise, nevertheless about 93% of all deaths did have an accompanying gross pathology. The majority of the necropsies were performed by only four prosectors, which ensured a high degree of consistency in the gross diagnoses. Of all the animals examined for gross pathology, only about 49% subsequently had a histopathologic examination, and this proportion varied among the studies (see Section 3).

### **2.3.3 Histopathology Codes**

As the pathologist read the slides, the diagnoses were recorded and coded on the bottom of the first page of the necropsy report. The MICRO dictionary of the four-letter histopathology codes is given in Appendix H.

All histopathological findings were classified as either lethal (L), contributory (C), or noncontributory (N). These findings may or may not have confirmed the decision made on the gross findings. The coded diagnoses were transferred to the third page of the necropsy report. This coded information was entered into the computer MICRO records for the experiments.

Histopathology was performed by several pathologists over the years. L.S. Lombard, a board-certified veterinary pathologist, was involved throughout the JANUS series, except for JM-14, and she performed the majority of the histopathological evaluations. Dr. Lombard died in 1987.

J.H. Rust, DVM, carried out many evaluations for the earliest studies, such as JM-2, -3, and -4. R.J.M. Fry also performed both gross and histopathological evaluations in the early years of the programs, before he took a position at the Oak Ridge National Laboratory in late 1977.

In the MICRO Dictionary (Appendix H), the content and codes were jointly developed by Drs. Fry, Lombard, and Rust. One might say the dictionary was developed iteratively during the late 1960s and early 1970s, and it reflects the cumulative experience of the three pathologists plus the pragmatic need to codify the principal pathology seen in the mouse in a reasonably simple and descriptive manner.

## **2.4 RECORD KEEPING AND DATA MANAGEMENT**

Computerized record keeping and data management reached a high level of development for the JANUS program. This capability evolved over the many years preceding the program; in a sense, it started with the earliest studies in the 1940s. It resulted from the fortunate confluence of skills, needs, and opportunities. The capability reached its highest form in the JANUS program, and it is being used as a role model for other DOE animal research programs. In 1988, the JANUS database was transferred from the ANL IBM mainframe to the ORACLE relational database management system. The use of ORACLE has permitted the JANUS data to be articulated with other ORACLE databases, such as that from the studies at ANL with the beagle.

The ORACLE system is organized into tables that contain all the information necessary to initiate experiments, to enter experimental data, or to be used in data analysis. Appendix I contains a list of the ORACLE tables and the definition of the fields in each table. Tables GENERAL, EXIT, FRACTIONS, MACBASE, MACFIND, MICBASE, and MICFIND contain all of the data for JM-2 through JM-14. The other tables are used in the initiation of new experiments. The computer-managed aspects of the JANUS experiments and data analysis are set into operation by the use of menu selections. These menu items are primarily for experimental setup, data entry, and data analysis, but with a little instruction, the database may be queried directly.

### **2.4.1 Data Entry**

The hard-copy records and codes presented in Appendices A, B, C, E, and H were used for data entry as described in Sections 2.2 and 2.3. The data were routinely entered into the appropriate tables by use of the menu. As every individual mouse was uniquely coded for experiment, radiation quality, sex, treatment, replicate number, cage number, and

individual number, entries into the database were internally controlled against random error. Nevertheless, all entries were subject to a quality control follow-up performed by a second party who was not involved in the original entry.

#### 2.4.2 Specialized Data Organization

For special applications, data from the tables may be merged for analysis. It is also necessary to have the radiation protocol codes for each experiment in the JANUS series available for use in a separate file (Appendix J). Users can thus select data for analysis by any array of codes for experiment, radiation quality, sex, and dose. Additional data may be extracted into separate files for special use.

The MACRO and MICRO codes have been grouped into MACRO and MICRO combined pathology glossaries (Appendices K, L, and M). These glossaries are used in analyses of the occurrence of pathological conditions. To compare the incidence of different diagnoses, there is a need to group similar diagnoses. Grouping similar findings can increase numbers as some individual diagnoses are not very plentiful and therefore not significant. Each of the combined pathology glossaries <E>, <F>, and <H> comprises 28 groups of definite composition: a group may be composed of 1) cause of death undetermined, 2) tumors or nontumors, 3) primary or secondary (metastatic) tumors, 4) like tumor types, 5) individual tumor type, 6) tumors of like tissue type, 7) tumors of specific organs or organ systems, 8) metastatic tumors, 9) metastatic tumors of specific sites or of specific origin, 10) nontumors, or 11) nontumors of specific organs or organ systems. Glossaries <E>, <F>, and <H> may have some groups in common but for the most part are different.

Glossary <E> contains all the possible codes in the dictionaries divided into the 28 groups: 3 major classes of connective tissue tumors, 13 classes of epithelial tissue tumors, 4 classes of secondary tumor occurrences, 7 classes of non-neoplastic disease, and 1 class of undetermined cause of death. One important use for this glossary, made possible by the singularity of each code, is in the analysis of concordance and discordance between gross and microscopic pathology. The specific contents of <E> are found in Table 1 (tables begin on p. 43) and Appendix K.

Glossary <F> regroups some components and subdivides others found in <E>. This glossary contains only tumor diagnoses, as over 75% of the cause-of-death diagnoses are a neoplasm. The contents of <F> are listed in Table 2 and Appendix L.

The third combined pathology glossary <H> (Table 3 and Appendix M) contains some groups repeated from <F> but has separated some classes of lymphoreticular tumors, connective and epithelial tissue tumors, and selected metastatic tumors in order to make more detailed comparisons of these diagnoses.

The use of the glossaries allows for the creation of a combined pathology database for each of the JANUS experiments. The combined pathology database contains each individual mouse scored for the occurrence of a diagnostic code found within the 28 groups.

A different database may be constructed for MACRO and MICRO diagnoses found for Glossaries <E>, <F>, and <H>. These databases are used in conjunction with the JANUS radiation protocol (Appendix J) in many of the analysis procedures.

### **2.4.3 Reliability and Potential Use of the Pathology Data**

A summary of the 13 JM series studies, which will be described in detail in Section 3, is presented in Table 4. This table provides the total numbers in the three major categories of death records, gross pathology records, and histopathology records. Between 90% and 98% of all death records have an accompanying gross pathology record, while between 0% and 85% of the gross records have an accompanying histopathology record. Obviously, the gross pathology data have both uniformly and adequately sampled the death records. The reliability (and, therefore, the usability) of the gross pathology records becomes an important consideration for any comparative analysis.

The issue of reliability and consistency of the pathology data, as the data accrued over the years, escaped neither our attention nor the attention of outside reviewers. An independent audit of the gross and microscopic pathology records was therefore contracted and was performed by Pathology Associates, Inc., of Frederick, Maryland, in 1986. The complete radiation, death, autopsy, and pathology records were randomly selected for about 50% of the animals from the data for two experiments, JM-4K and JM-13. The results of the audit confirmed the consistency and repeatability of the gross diagnoses and of the judgments on the causes of death made by the prosectors. The pathologists performing the audit concurred with the gross and microscopic diagnoses in over 90% of the cases examined. This was considered an excellent level of agreement, and the auditors also acknowledged that some of the differences in opinion on cause of death were equivocal.

#### **2.4.3.1 Analysis of Concordance between the Gross and Microscopic Pathology**

As a consequence of the audit's findings, we established the principle that the histopathological findings could be held as the ultimate truth and used, therefore, to test quantitatively the level of concordance or agreement between the gross and microscopic pathology. As noted in previous sections, the gross pathology record always suggested a "cause of death," a lethal (L) tumor or other lesion, including an undetermined cause (CDU). The histopathology classified each finding as either lethal (L), contributory (C), or noncontributory (N). By grouping the histopathological findings as either lethal (L) or lethal plus contributory (LC), comparisons can be made with the gross finding of L to determine the accuracy of that original judgment. The comparison of the two L classes is straightforward. The test of gross L against histopathology LC broadens the basis of comparison and recognizes realistically that the gross finding has limitations that are somewhat alleviated by including the histopathologically defined lesions that are clearly contributory to the animal's death.

The concordance test for all observed pathology, that is, all observed gross diagnoses vs. all observed microscopic diagnoses (lethal plus contributory plus noncontributory, LCN), is essentially a test of the thoroughness and accuracy of the observations made by the prosectors at necropsy. It is not a test of judgment of the severity of a lesion, but rather, on its presence.

A summary of concordance analyses for a portion of the JM series (JM-2, -3, -4K, -4L1, -4L2, and -9) is given in Table 5 for selected single and grouped endpoints from pathology glossaries <E> and <F>. About 13,400 matched records are included in this summary. The level of concordance (percentage of gross diagnoses confirmed by histopathology) is presented for the three categories of L, LC, and LCN. Only tumor-related deaths and tumor occurrences were analyzed because these account for over 75% of all terminal pathology and causes of death.

Table 5 reveals that, at best, only seven gross pathology categories could be consistently used, on the assumption that the concordance rate should be 85% or greater. These categories are the underlined values in the table, and the best array is that under the LC column. In other words, a less rigid definition of cause of death that includes contributory lesions provides a good cross section of pathologies: three connective tissue groups, three epithelial tissue groups, and the all-inclusive class of "all primary tumors." The inclusion of tumors of the Harderian gland is of special note because this tumor is highly responsive to neutron exposure.

The all-observed-pathology analysis (LCN) does not materially improve the concordance rates, though many of the pathology groups do have significantly increased sample sizes. That fact, in turn, should improve statistical factors.

#### **2.4.3.2 Analysis of the Discordance between the Gross and Microscopic Pathology**

The test for discordance is an analysis of errors of judgment regarding the presumed cause of death defined by the prosector. This analysis can only be done for the lethal category with pathology glossary <E> for both gross and microscopic pathology, because the analysis requires a nonconflicting matching pair of diagnoses for each animal. The animal can only be represented by a single diagnosis for the gross and for the microscopic pathology. Multiple entries per mouse, as for the LC category, confuse the computer. In spite of limitations, the discordance analysis allows detection of patterns of error in the gross pathology that can be valuable in the interpretation of any analysis of the gross findings.

Although the analysis runs the full  $28 \times 28$  matrix, not all cells in the matrix have entries, and many have sample sizes too small to give useful information. Table 6 presents a selected  $7 \times 7$  matrix involving diagnoses that not only have adequate sampling but also produce information that reveals the nature or pattern of diagnostic errors. Simply stated, the errors are not random.

The undetermined cause category (CDU) is large, and the majority of discordant diagnoses became reclassified as lymphoreticular tumors. This latter class has a very small discordance rate, and most of these go to the CDU class. For the most part, misdiagnoses among connective tissue tumors are reclassified within that general category. On the other hand, errors among the epithelial tissue tumors (lung, liver, and ovarian tumors) are predominantly reclassified after microscopic study into the connective tissue diagnoses, mostly as lymphoreticular tumors. The reader should note that liver tumors have a high rate of discordance (about 50%) and nearly two-thirds become reclassified as lymphoreticular or vascular tumors. Thus, data from grossly detected liver tumors cannot be used with sufficient reliability to warrant the statistical effort.

As a final note, any reclassification to another type of tumor within the broad categories of either connective or epithelial tissue tumors is not as serious as a reclassification to the other category. For example, a lung tumor that is reclassified as a lymphoreticular tumor is of more concern than a vascular tumor reclassified as a lymphoreticular tumor. Dose-response and radiation quality factors are quite different for the two major categories.

## 2.5 ANALYTICAL APPROACHES

Although ORACLE is a powerful data management tool that permits the database to be easily transported to a variety of computer platforms and operating systems, its power also means that an elaborate and complex programming language exists between a researcher and the database. Consequently, an interactive menu-driven interface (MDI) on the computer system in the Center for Mechanistic Biology and Biotechnology was developed as an alternative to ORACLE for accessing the JANUS database. The MDI was designed specifically to be a flexible and easy-to-use tool for the researcher.

The philosophy governing the MDI has evolved through the years. Originally, the MDI provided options to perform such functions as regression analysis and the computation of various actuarial statistics. As new methods of analysis have constantly emerged, it was recognized that an analysis-oriented MDI would become progressively more complex and require constant vigilance over quality control in order to satisfy the demands of a changing set of researchers interested in the database. As a consequence, the generation of data files for subsequent analysis has become the primary function of the MDI today. One philosophical element of the MDI has remained invariant: the MDI provides access to the database, but it does not permit the database itself to be modified.

Age at death (failure time) is a fundamental unit of information in any study designed to investigate the biological effects resulting from exposure to radiation. Quantitative methods used to analyze failure times can be divided into either those that require individual death times or those that require the death times of individuals to be grouped into discrete time intervals. The MDI for the JANUS database provides the researcher with the option to select either of these two formats for data output. In the

discrete case, the MDI also allows the specification of a fixed interval width format for the output file or an output file organized by user-defined intervals of varying widths.

The MDI database provides several additional capabilities for the analysis of failure times. For example, treatment codes (see Appendix J) can be provided during the dialog session to select the dose groups, exposure patterns, or radiation qualities that will be included in the output file. Gender-specific selections for individual dose groups in the output file can also be made.

Methods for failure-time analysis can also be subdivided into those used to analyze data on "cause of death" and those used to analyze data on incidence or prevalence. The MDI addresses the data requirements for these types of analyses by requiring the researcher during the dialog session to specify whether the data for the output file are for lethal events only (L), lethal plus contributory events (LC), or any observed pathology (LCN). It is also necessary to specify whether the data being output should be based on observations made at necropsy (gross pathology) or by histopathologic examination. As not all animals underwent histopathological examination, an option also exists to generate analysis files containing histopathology data for those mice where this information is available and gross pathology data for those mice lacking histopathology diagnoses.

When a specific cause of failure is the focus of an analysis (e.g., death resulting from a specific neoplasm), it is necessary to identify the subset of animals that died of the event of interest. When ungrouped data is being generated, those pathology endpoints considered events (lethal, or lethal plus contributory) for a mouse are set to unity and the pathology variables for non-events are set to zero. For grouped data, the selection of lethal or lethal plus contributory determines how the count of events for each pathology endpoint is computed.

In order to perform analyses, the codes used to describe specific pathologic events in the JANUS studies have been merged into three larger assemblages called combined pathology glossaries (Appendices K, L, and M). Each file generated by the MDI can contain up to 28 groups of these combined pathology codes. If the need arises, new databases can be created from combined pathology glossaries tailored to the specific research interests of the investigator. Once created, the new databases can be automatically accessed within an MDI session. The only restriction imposed on the researcher is that the analysis files generated through the MDI cannot contain more than 28 groups of pathology codes.

The MDI for the JANUS database is so easy to use that it can quickly lead to a proliferation of analysis files, which under typical work environments could lead to confusion over what information is actually contained in a given file. Fortunately, the MDI provides an automatic audit trail through the convention used to assign names to every file generated. Every file name begins with "LIFE" and ends with a five-digit number that provides a running count of the number of files that have been generated by the MDI. The data files are given the extension SIN (e.g., LIFE00932.SIN) and come paired with an IDX file (e.g., LIFE00932.IDX) that provides an index of the pathology versions and treatment group selections specified in the dialog session. In addition, a batch (extension BAT) file is created

to actually generate the analysis files when a normal termination of the MDI session occurs. This batch file also contains an echo of the responses given in the MDI session. The MDI, therefore, allows an investigator to go back and determine exactly when a file was created, what it was called, and what information is contained within that file.

At present, direct access to the JANUS database is restricted to authorized personnel at ANL. However, access to analysis files generated from the database is available via collaborative arrangements with staff members in the Center for Mechanistic Biology and Biotechnology. Arrangements are currently being made to transfer an electronic version of the entire animal database to the National Radiobiology Archive, an organization at Pacific Northwest Laboratory charged with the Department of Energy (DOE) mandate to archive and provide public access to data generated from animal studies funded by DOE.

### 3 THE JANUS PROGRAM EXPERIMENTS

#### 3.1 INTRODUCTION

The JANUS program was first conceived in mid-1958 and subsequently went through a series of modifications and reevaluations. Generally, the plans tended to be grandiose, with the predictable criticism that the program would not be able to achieve programmatic goals either quickly or inexpensively. The program that ultimately emerged is probably best defined in Grahn et al. (1972) in a simple statement:

The primary program objectives are to obtain data for the development of realistic models of chronic radiation morbidity and mortality whereby long-term radiation injury can be understood and predicted in terms of: (1) cell injury and recovery; (2) tissue and organ injury, repair and regulation; and (3) the actuarial statistics of disease and death.

These goals were not beyond reach, but in many respects, they were not fully achieved generally because funding levels were not adequate, and the need for compromise prevailed. This archive contains the "actuarial statistics" and the associated pathology. There is no equivalent archive of the many studies done on hematology, immunology, cell injury and repair, and other areas, including dosimetry. Much of the work concerning nonactuarial data has been published, and a list of publications from the JANUS program is appended to this document (Appendix N).

#### 3.2 THE JANUS (JM) SERIES

##### 3.2.1 JM-2

JM-2 was the first, the largest, and the most ambitious of the JM series. One necessary objective was to test the additivity of small increments of neutron dose, when given in different patterns of exposure over a 24-wk period. With use of five different exposure patterns (Table 7 and Appendix J), a common total neutron dose of 240 cGy was delivered. These ranged from a high-dose-rate single exposure to a fractionated exposure given in three low doses per week for 24 wk. A matching set of  $\gamma$ -ray exposures delivered a total dose of 855 cGy in 24 wk and a 788-cGy single dose. These  $\gamma$ -ray and neutron exposures compared the influence of changes in dose rate, in the number of fractions, and in the protraction period on the long-term response. A three-dose/single-dose series was also included along with a matching set of sham-irradiated controls. This test of exposure patterns was important for future planning because the JANUS facility could not be used, for logistical and economic reasons, for 5-7 d of irradiation per week for 6-8 h/d as had been done in our earlier studies with  $\gamma$  rays (Grahn et al. 1994).

The important objective was to evaluate the influence of these different exposure regimes on the endpoints of life shortening and neoplastic disease incidence and, in turn, on the estimation of RBE values. Sample sizes per sex, dose, and exposure pattern were sufficient to yield accurate estimates of the life table and pathology at death.

It was well known from previous studies that fractionation of a  $\gamma$ -ray dose would reduce its effectiveness, but the characteristics of specific exposure parameters were critical to the magnitude of this dose-rate effect. We were obliged to match every neutron pattern with  $\gamma$ -ray irradiations and were uncertain as to the additivity, or the magnitude of any deviations therefrom, of the neutron exposures. The choice of 24 wk was a compromise that permitted an adequate protraction period (about 20% of the control mean after-survival [MAS]) yet also permitted a large and necessary experiment to be executed over a reasonable period. In fact, 10 full replications, involving a total of over 11,000 mice, were completed between March 1971 and June 1972.

A small age-dependence test was also included in JM-2. This involved two single doses of neutrons and of  $\gamma$  rays given at about 200 and 300 d of age, spanning the 24-wk (168-d) fractionation period from 100 to 268 d of age. The single doses matched those given at 100 d of age.

No new studies were initiated until March 1974. This 2-yr hiatus permitted the Gammabeam 650 irradiator to be installed in the HLGf. The JM-2 data also accrued in this period to provide guidance for the next series of studies, JM-3, -4K, -4W, -7 and -8, which were initiated in the spring and summer of 1974.

The results of JM-2 were presented in an interim status by Ainsworth et al. (1974, 1976) and in a more complete form by Thomson et al. (1981a). An important finding was the nonlinear response, in terms of life shortening, to the single neutron doses of 20, 80, and 240 cGy. The response was concave downward, with the effect at 20 cGy being about 4-fold greater per centigray than at 240 cGy. The 24 weekly fractionation procedure at 240 cGy augmented the life-shortening response from about 1 d lost per centigray to about 1.5 d. This type of dose- and fractionation-dependent response to neutrons, opposite to that seen for  $\gamma$ -ray irradiation, was an important consideration in program planning.

With regard to dose additivity for individual neutron exposures, there was no significant difference between the response to three exposures per week of 15 min each and one per week for 45 min. Similarly, there was no difference in the response to one neutron exposure per week for 45 min and one per week for 360 min. However, one exposure per 4-wk period for 180 min per exposure did cause a shift in response for both  $\gamma$  rays and neutrons, but in opposite directions. The six larger once-monthly  $\gamma$ -ray increments were more effective than the smaller weekly exposures, while the opposite effect was noted for neutrons; the smaller weekly increments were more damaging. As a consequence of these results, all subsequent long-term neutron exposures employed the once-weekly, 45-min exposure paradigm, though there were some exceptions. Exposures to  $\gamma$  rays matched the neutron exposures.

### 3.2.2 JM-3

This was a straightforward single-dose study composed of seven replications that were run between April 1974 and June 1977. A small dose-rate comparison was also included in the last replication. It involved a single dose of 240 cGy of neutrons given to males only. One group was exposed for the usual 20 min, and a second group was exposed for 8 h. Table 8 gives the full inventory and dose array for JM-3. Because of funding constraints, only about one-half of the originally intended number of females were included in the final inventory. Some were discarded after about 1 yr, and others were simply not entered in the study. However, as with JM-2, both MACRO and MICRO pathology records are quite complete in relation to the number entered.

The reason the entries into this study were stretched out over 3 yr was due to competition for the available experimental animals. Concurrent with JM-3, five other studies were also being carried out, as will be noted.

### 3.2.3 JM-4

There are four experiments under the JM-4 rubric (we acknowledge this happenstance to be one of our few coding errors). The data are given in Tables 9 and 10, as well as in Appendix J. The basic study is known as JM-4K, as per the treatment codes for the total doses given in Table 9, and it involved the 24 once-weekly exposure procedure that was employed in JM-2. Irradiations were carried out in 10 replications between August 1974 and April 1977. Some of the total doses were repeated in JM-3, JM-4L1, and JM-7 to provide a more direct test of dose-rate and protraction factors. The study was done concurrently with JM-3, JM-7, and JM-8.

Another concurrent study was JM-4W, which only employed females and two total dose levels each for  $\gamma$  rays and neutrons (Table 9). The study, done in six replications between June 1974 and June 1978, was intended for a sacrifice-series study of vascular damage, which was carried out, but the original sample sizes were more than adequate (see Table 9) so that excellent survival data became available. No histopathology was performed; however, there are complete records for the gross findings.

The two studies listed as JM-4L (Table 10) were done in the early 1980s, 3-5 yr after the JM-4K study was executed. The first of these, JM-4L1, was originally intended to be carried out in parallel with JM-4K, as it involved four of the same total doses used in that study. The study involved  $\gamma$ -irradiated males only, and the protraction period was 23 wk, the same elapsed time for the 24 once-weekly procedure of JM-4K. Dose rate was reduced by a factor of about 150 in the JM-4L1 study. Total doses were delivered over a 22-h day, 5 d/wk for the 23 wk (6600 min of exposure per week vs. one 45-min exposure per week). No comparable neutron exposures were possible. Irradiations were done in four replications between November 1980 and June 1981.

The second low-dose-rate study, JM-4L2, was planned to parallel the JM-13 study, which involved a 60-exposure, once-weekly regime. The JM-4L2 experiment employed the same exposure procedure as JM-4L1, but it extended the protraction period to 59 wk, the elapsed time for the 60 once-weekly exposures. Again, only males were used, and no neutron exposures could be done to match the  $\gamma$ -ray irradiations. Five replications were exposed between July 1983 and October 1984.

The exposure, caging, and animal handling procedures had to be different for these two low-dose-rate studies. These were described in Section 2.2. The irradiations were performed in the low-level  $\gamma$ -ray facility previously described in Grahn et al. (1994). A portable Gammabeam 150 irradiator with a single  $^{60}\text{Co}$  source was used for the irradiations. Dose rate was controlled by distance from the irradiator, which was located in an off-center position in the room. A constant exposure day of 22 h, 5 d/wk, was used throughout the two studies. Both studies used the same three lowest weekly total doses, 8.96, 18.13, and 41.7 cGy/wk, but source decay prevented our being able to accommodate a fourth dose in JM-4L2 at 4-5 cGy/wk and still include the highest level.

The source-handling mechanism described in Grahn et al. (1994) had been decommissioned in the late 1970s and was replaced with the "portable" Gammabeam 150 unit, originally fitted with a 6- to 8-Ci  $^{60}\text{Co}$  source. This unit was used for both JM-4L experiments. There were no unusual dosimetric aspects, so the same kerma-to-midline-tissue-dose parameters were used as in the HLGf.

### 3.2.4 JM-7

JM-7 (Table 11) used a 60-exposure, once-weekly procedure (treatment code Q) to extend the protraction period to approximately 50% of the normal life expectancy from 100 d of age, when the weekly exposures were initiated. This experiment used only two total doses each for  $\gamma$  rays and neutrons, and these matched two that were used in JM-4K. One  $\gamma$ -ray dose and both neutron doses were also a repeat of JM-3, and both  $\gamma$ -ray doses were repeated in JM-4L1. To evaluate the age-at-exposure variable, JM-7 also included a single-dose component (treatment code R) at approximately 520 d of age, the end of the 60 once-weekly series. Two doses each for  $\gamma$  rays and neutrons were used, and these matched doses used in JM-3 and JM-4.

The 60-week series involved 10 replications over the period from March 1974 to July 1978. The six replications of the single-dose test were irradiated between April 1975 and April 1977. These replications were from an unexposed portion of the first six replications of the 60-week series. They were then irradiated on the same date as the last of the 60 weekly exposures.

### 3.2.5 JM-8

This was the only duration-of-life exposure experiment done in the JM series. It was ostensibly intended to link the JANUS program to the extensive duration-of-life studies done in pre-JANUS experiments (see Grahn et al. 1994) and to compare protraction factors between the 24 and the 60 once-weekly paradigms with the duration-of-life procedure.

The exposures were given once weekly, as in the 24- and 60-wk studies, and three weekly dose levels were used for both  $\gamma$  rays and neutrons. The weekly dose levels are found in Table 12. Mean total doses would be the product of these weekly doses and the mean number of weeks of survival. The lowest and highest weekly doses of the three, for both  $\gamma$  rays and neutrons, were the same weekly doses used for the JM-7 60 once-weekly series, which tied these two experiments together. The middle dose levels, 17.4 and 1.67 cGy/wk for  $\gamma$  rays and neutrons, respectively, were the same rates used in JM-4K to reach total doses of 417 and 40 cGy in 24 wk of exposure. Between 1 and 10 replications were used, and these were initiated between April 1974 and May 1980. Sample sizes for the females were not adequate for most dose groups but were sufficient for males.

### 3.2.6 JM-9

Owing to administrative and budgetary changes in mid-1977, experimental priorities changed. One change was the more pressing need for truly low-dose studies, especially with neutrons, because of accumulating evidence that higher levels of damage per centigray were induced at doses below 20–40 cGy as compared with that at doses above that level. The JM-9 experiment developed from this background. It consisted of two phases (Table 13). The first was a preliminary study carried out between June 1977 and March 1978 and was composed of only five replications. Only two neutron dose levels were used, 5 and 10 cGy. The latter was delivered in both the single dose and the 24 once-weekly regimes.

The second phase was performed with 10 replications between February and August 1980. Though restricted to the female, it was a large study that used larger sample sizes at the lowest doses than had been used in any previous studies. An excellent gross pathology file was created, and about 40% of the mice had a histopathology follow-up. This study also provided the first good example of an essentially null response dose, the 1-cGy neutron dose.

### 3.2.7 JM-10

From the outset, the JANUS program intended to include studies that compared the responses of several species, though the primary species was always to be *Mus musculus*, the mouse. Plans included studies with beagles, guinea pigs, and several species of wild mammals that had been captured and established in breeding colonies in the ANL animal facilities. The original intention was to provide a multiple-species database for comparisons that would enable an improved interspecies modeling effort, with the ultimate goal of predicting human responses to neutron and  $\gamma$ -ray exposures. The usual funding, manpower,

and programmatic deficiencies limited this interspecies comparison effort to one laboratory-maintained, long-lived field mouse, *Peromyscus leucopus* (see also Section 2.1.1.2).

The exposures of *P. leucopus* were done between November 1977 and March 1979 in 10 replications. Only males were employed. The dose levels were repeats of those used in JM-3 and JM-4K. Single exposures to both  $\gamma$  rays and neutrons were employed, and two total dose levels of neutrons were given in the 24 once-weekly procedure (Table 14, treatment codes VV and VW).

As shown in Table 14, the control MAS for *P. leucopus* is about 50% longer than that of the B6CF<sub>1</sub> mouse, though body size was not that much greater. In general, the response in terms of life shortening was not particularly different from that of the B6CF<sub>1</sub> mouse, but a different spectrum of pathology was seen at death. No histopathology is available, however.

### 3.2.8 JM-12

A curious aspect of the response to neutrons concerns the so-called reverse dose-rate effect; that is, as neutron doses are protracted or fractionated, life shortening (among other responses) is augmented. This was seen in JM-2 and in the comparison of JM-3 with JM-4K. A small study, JM-12 (Table 15), was carried out to test the relationship of this augmentation phenomenon to the short-term fractionation of dose specifically, by delivering a given total dose in only 1, 2, 4, or 6 fractions at 1-wk intervals. Only males were used, and the irradiations were carried out in six replications between November 1979 and April 1980. Though no histopathology was done, the gross pathology record is complete.

### 3.2.9 JM-13

The last major study of the life-shortening and pathologic responses was the JM-13 experiment (Table 16). In contrast to all previous studies, JM-13 was not funded by the U.S. Department of Energy (DOE). It was fully funded by the U.S. Nuclear Regulatory Commission (NRC), which was concerned about the potential risks associated with the periodic exposure of utility workers in the nuclear power industry to fission neutrons, especially at pressurized-water reactor facilities. The lowest total neutron dose of 2 cGy, delivered in 60 once-weekly exposures of 20 min each, required a dose rate of only 0.00167 cGy/min. This was achieved with a high degree of reliability.

Another unique feature of the JM-13 study was the inclusion, from concept to completion, of a series of periodic genetic evaluations of males drawn randomly from the control and irradiated groups during the course of the exposures. The paradigm of 60 wk of exposure was chosen as it was a reasonable approximation of a working lifetime for persons in the industry. Sixty weeks is also about 50% of the MAS for a young adult mouse. This would be roughly equivalent to a 30- to 40-yr period starting at 20 to 25 yr of age for a human population in the United States.

A concurrent issue at the time JM-13 was being executed (February 1981 to August 1982 for the exposure sequence) was the "quality factor" (Q) or, experimentally, the RBE for neutrons at very low doses delivered at low dose rates. The accepted value of 10 for fission neutrons was believed by many to be an underestimate. We expected JM-13 to make a significant contribution toward the resolution of this concern about the neutron RBE, because the study was addressing both somatic and genetic responses to low total neutron doses (<10 cGy) delivered at extremely low rates.

Table 16 indicates that, on average, only about 50% of the autopsied animals were subject to a histopathological examination. This level of pathology study was set by agreement with the NRC, the funding agency.

### **3.2.10 JM-14**

JM-14 (Table 17) was the last major study of the JANUS program, now under the leadership of D.J. Grdina. Funding for this experiment was divided among the DOE, the National Cancer Institute of the National Institutes of Health, and the Center for Radiation Therapy of the University of Chicago. The primary purpose was to evaluate the efficacy of several radioprotector agents against the induction of late effects, specifically life shortening and tumorigenesis. The agents were WR-2721 [S-2-(aminopropyl-amino)ethylphosphorothioic acid] and WR-151327 [S-3(3-methylaminopropylamino)propyl-phosphorothioic acid].

The study used single doses of  $\gamma$  rays and neutrons at levels previously employed in the program (JM-3, JM-9). Animals were injected intraperitoneally 30 min before irradiation with either the radioprotector or saline. The irradiations were carried out between October 1984 and October 1985. At this time, the histopathology record is incomplete; however, a complete gross pathology record is in the file.

## 4 SUMMARY

### 4.1 INTRODUCTION

A complete review of all results of the long-term effects of whole-body  $\gamma$ -ray and neutron irradiations performed in the JANUS program cannot be given here. Instead, this brief summary will identify the major findings and, also, some of the unresolved issues as we currently see them. The results are presented in more complete form in published articles (see Appendix N), but there is no single summarizing published report. At the writing of this report (late 1994), there are still portions of the data that have not been fully analyzed and, in some cases, that have not been analyzed at all. A quick introduction for the reader to the life-shortening data of the individual JM experiments can be found in the following references:

JM-2	Ainsworth et al. (1976); Thomson et al. (1981a)
JM-3	Thomson et al. (1981a)
JM-4K,-4W	Thomson et al. (1981a)
JM-4L1, -4L2	Thomson and Grahn (1989)
JM-7	Thomson et al. (1981b)
JM-8	Thomson et al. (1981b)
JM-9	Thomson et al. (1983, 1985b)
JM-10	Thomson et al. (1986)
JM-12	Thomson et al. (1985a)
JM-13	Thomson and Grahn (1988)
JM-14	Grdina et al. (1991a,b); Carnes and Grdina (1992)

Comprehensive analyses and modeling of life-shortening effects are in Carnes et al. (1989) and Carnes and Grahn (1991). A summary and analysis of major tumorigenic responses are in Grahn et al. (1992). A combined, but incomplete, summary of genetic, life-shortening, and tumorigenic responses was published earlier in Grahn et al. (1986).

### 4.2 THE NEUTRON/GAMMA-RAY RBE

Obviously, there is no single best estimate of the RBE. The major variables that influence the RBE value are discussed in the following sections.

#### 4.2.1 Sex

There is no specific sex-related factor influencing the RBE that cannot be related to sex-specific tumor incidence or death. While there are sex differences in neoplastic disease incidence, there is no significant sex difference in overall life shortening per unit dose.

#### 4.2.2 Total Dose/Dose Rate/Protraction Period/Fractionation Pattern

One always wishes that the dose variables could be stratified to bring out the specific contributions of each variable. Unfortunately, they are a matrix of interdependent variables, and the JM series certainly did not exhaust the options. In terms of life-shortening estimates per cumulative dose (centigray), the RBE for single, low neutron doses would be about 10 ( $-4$  d/cGy of neutrons vs.  $-0.4$  d/cGy of  $\gamma$  rays), but this RBE would drop to 5 or less as the neutron dose goes above 40 cGy. Assuming complete additivity of small increments of neutron doses accumulating to 10 cGy or less, the RBE would range between 25 and 40 against comparable  $\gamma$ -ray exposures. Neutron effectiveness is lower per centigray at doses above 40 cGy than at doses of 20 cGy or less, regardless of exposure parameters.

For  $\gamma$  rays, decreasing the dose rate, increasing the protraction period, and reducing the size of a dose fraction all act to diminish life-shortening effects. The "round numbers" for this series of experiments, the number of days lost per centigray of  $\gamma$  rays, are as follows:

single dose	0.40	23 wk, 5 $\times$ 22-h days	0.16
24 weekly doses	0.20	59 wk, 5 $\times$ 22-h days	0.08
60 weekly doses	0.14	duration-of-life, weekly dose	0.09

The life-shortening effect of daily duration-of-life exposure to  $\gamma$  rays for 8 h/d is 0.04 d per cumulative centigray at doses less than 20 cGy/d, as was seen repeatedly in the pre-JANUS studies at ANL (Grahn et al. 1994). Thus, while the maximum n/ $\gamma$  RBE in the JM series is about 50 (4.0/0.08), it would be 100 (4.0/0.04) if the pre-JANUS studies at ANL were used as the low-LET baseline.

#### 4.2.3 Dose-Response Functions

There were no unusual dose-response functions for any of the long-term somatic or genetic endpoints. The response to  $\gamma$  rays was predominantly linear, regardless of the exposure variables involved. Not only were they usually linear, but they uniformly extrapolated close to the 0,0 intercept. The occasional response was linear-quadratic, a second degree polynomial with a positive dose-squared term.

For neutron exposures, the responses were mixed. Depending on the range of total doses involved, they were either linear or linear-quadratic, with a negative second-degree term.

A variety of dose-response models were evaluated, but the simplest models prevailed (Carnes et al. 1989). RBE values were therefore easily derived from the ratio of linear terms,  $\beta_n/\beta_\gamma$ .

#### 4.2.4 Age at Exposure

This variable was only tested with single doses at three ages greater than the standard age of  $100 \pm 15$  d. The three ages were approximately 200, 300, and 500 d of age. The RBE value at the older ages was not substantially different from that at 100 d of age at exposure when measured in terms of the life-shortening response. Life shortening itself was dependent on age at exposure. In terms of days lost per centigray, the values for  $\gamma$  rays were 0.5, 0.3, 0.2, 0.2, for 100, 200, 300, and 500 d of age at exposure, respectively; for neutrons, the values were 1.0, 0.6, 0.3, and 0.5. These rather low values for neutron exposures were due to the unfortunate choice of dose levels (40 cGy up to 240 cGy), where the life-shortening effect steadily diminishes with increasing dose.

Though these data did not have a specifically identified control group from which the after-expectations of life could be derived for each age-at-exposure group, reasonable approximations can be made from other controls. The diminishing life-shortening term is probably reasonably accurate; however, the data also reveal that this phenomenon is likely to be a reflection of a reduction in age-specific tumor-related death rates at fixed age intervals as age at exposure increases. Latency may not be shortened as age at exposure increases, and tumor yields may be similar at comparable elapsed time periods after irradiation. These elapsed time periods, when converted to ages, reveal that tumors occur progressively later in life and thus have less influence on life shortening. These data need further analysis.

#### 4.2.5 Endpoint

Obviously, RBE values are dependent on the endpoint. In general terms, the RBE values for life shortening are the best estimates for overall somatic effects, because life shortening at low doses principally reflects excess mortality attributable to neoplastic disease. The maximum RBE values occur at low doses, where about 85% or more of the life shortening can be attributed to excess tumor-related mortality. Within the broad class of neoplastic disease, however, considerable heterogeneity exists in the induction rates for different types of tumors for the two radiation qualities.

Epithelial tissue tumors are induced by neutrons at higher rates per centigray than are connective tissue tumors. The lowest RBE value,  $2 \pm 0.3$ , is thus seen for lymphoreticular tumors induced by single doses, and the highest significant values are between 50 and 100 for tumors of the liver, Harderian gland, and other glandular and reproductive system tumors, except for those of the ovary. The RBE range for life shortening is between 5 and 45, depending on the dose-rate factors that parallel the same range for tumorigenesis. This range of RBE values and its relationship to dose-rate and fractionation factors is also seen in the cumulative induction of reciprocal chromosome aberrations in the stem cells of the male germ line.

### **4.3 UNRESOLVED ISSUES**

No series of experiments in radiation biology has ever succeeded in solving all the problems it set out to resolve, and, usually, a new set of problems is created. The JANUS program was no different from other experiences.

#### **4.3.1 Dose-Response Functions**

There remains a need for more data on the responses to  $\gamma$  radiation at doses between 5 and 50 cGy for both sexes. Similarly, the data from neutron exposures at 2–20 cGy need to be reinforced equally for both sexes. While we believe the response to  $\gamma$  rays is linear at low doses and will continue to extrapolate to the 0,0 intercept, this assumption needs more support. For neutron irradiations, the essentially linear response, through the intercept, at doses between 1 and 20 cGy needs to be confirmed for both sexes with a broader variety of dose-rate and fractionation factors.

#### **4.3.2 Dose Rate, Fractionation and Protraction Factors**

The JM series left some gaps in this area. Dose-response data for both sexes were not balanced, and the short-term 24 once-weekly sequence was particularly not satisfactory. The one duration-of-life series left unanswered the matter of bridging the databases from the pre-JANUS studies with those of the JANUS studies. The once-weekly duration-of-life procedure was twice as effective for life shortening than the daily, 8 h/d, duration-of-life procedure for  $\gamma$  radiation. The neutron duration-of-life series, unfortunately, did not go to a low enough total dose, so the response to lifetime accumulations of less than 20–40 cGy remains unanswered, though we would predict it would converge on the responses to the short-term exposure parameters that were employed.

#### **4.3.3 Age at and during Exposure**

This issue encompasses problems of long standing in radiobiology: Why do responses seem to lessen with increasing age, and why does the concept of "wasted radiation" still find adherents? The JM series noted that responses to  $\gamma$  rays declined from 1 to 24 to 60 wk of exposure and that a lower instantaneous dose rate within the 24 and 60 procedures also had a reduced effectiveness. There was a significant difference between 60 once-weekly and duration-of-life once-weekly, but no difference appeared between the latter and exposures for 59 weeks, 22 h/d for 5 d/wk. Nevertheless, both procedures were still twice as effective as daily duration-of-life exposures for 8 h/d. Obviously, radiation cannot be "wasted" in the sense that it truly lacks any effectiveness. Depending on the endpoint, effectiveness diminishes under certain long-term exposure conditions, and this remains to be rationalized.

#### 4.3.4 Neoplastic Diseases

Several issues that relate to tumor incidence and mortality have yet to be addressed in this database. One concerns the question of tumor multiplicity, that is, are there important radiation quality, dose, sex, and age factors that may be manifest in the occurrence of two or more neoplastic conditions in the same animal? Another issue concerns the degree of malignancy of induced tumors and its relation to the noted variables. This could be addressed by a careful survey of metastatic tumors. A third concern relates to the variability in tumor induction that may be conditioned by genetic background. As the JM series used only one F<sub>1</sub> hybrid mouse, which was characterized by a high spontaneous frequency of both lymphoreticular and lung tumors, there is somewhat limited information on the full spectrum of tumors that might be seen and on their rates of induction, dose-response parameters, and RBE values.

#### 4.3.5 Other Issues

The circumstance wherein groups exposed to low doses, low dose rates, or both have an MAS greater than their specific controls (the "hormesis" issue) was not a problem in these studies. There were three cases of "over-survival," all nonsignificant. These were, in terms of life shortening, JM-3: 0 vs. 90 cGy of  $\gamma$  rays, females,  $-5 \pm 20$  d; JM-9: 0 vs. 1 cGy of neutrons, females,  $-2 \pm 10$  d; and JM-13: 0 vs. 2 cGy of neutrons, males,  $-9 \pm 11$  d.

The 90- and 2-cGy groups both showed a deficit in the cumulative risk of lymphoreticular tumors, a dominant cause of death in the B6CF<sub>1</sub> mouse. Both groups also showed an excess risk for epithelial tissue tumors, many of which are classed as contributory or nonlethal. The 1-cGy neutron group of females was an almost exact replication of its control for all causes and all dominant pathology. In other words, this instance is the closest to a threshold exposure in our experience. Even the ovarian tumor incidence was unchanged from the control, but there were small excess risks at 1 cGy for lymphoreticular, kidney, gastrointestinal, adrenal, and Harderian gland tumor occurrences. Thus, while life shortening may seem to show an hormetic effect, many specific tumor occurrences will demonstrate radiation injury, as will the germinal tissues.

## 5 REFERENCES

- Ainsworth, E.J., R.J.M. Fry, P.C. Brennan, S.P. Stearner, J.H. Rust, and F.S. Williamson, 1976, Life shortening, neoplasia, and systemic injuries in mice after single or fractionated doses of neutron or gamma radiation, in *Biological and Environmental Effects of Low-Level Radiation*, vol. I, International Atomic Energy Agency, Vienna, pp. 77-92.
- Ainsworth, E.J., R.J.M. Fry, D. Grahn, F.S. Williamson, P.C. Brennan, S.P. Stearner, A.V. Carrano, and J.H. Rust, 1974, Late effects of neutron or gamma radiation in mice, in *Biological Effects of Neutron Irradiation*, International Atomic Energy Agency, Vienna, pp. 359-379.
- Bennett, E.F., and T.J. Yule, 1972, A neutron spectrum map of the JANUS irradiation facility using proton-recoil proportional counters, *Radiation Research* 50:219-233.
- Borak, T.B., and T.G. Stinchcomb, 1979, Calculations of charge-particle recoils, slowing-down spectra, LET and event-size distributions for fast neutrons, and comparisons with measurements, *Physics in Medicine and Biology* 24:18-36.
- Carnes, B.A., and D. Grahn, 1991, Issues about neutron effects: the JANUS program, *Radiation Research* 128:S141-S146.
- Carnes, B.A., D. Grahn, and J.F. Thomson, 1989, Dose-response modeling of life shortening in a retrospective analysis of the combined data from the JANUS program at Argonne National Laboratory, *Radiation Research* 119:39-56.
- Carnes, B.A., and D.J. Grdina, 1992, *In vivo* protection by the aminothiols WR-2721 against neutron-induced carcinogenesis, *International Journal of Radiation Biology* 61:567-576.
- Grahn, D., E.J. Ainsworth, F.S. Williamson, and R.J.M. Fry, 1972, A program to study fission neutron-induced chronic injury in cells, tissues, and animal populations, utilizing the JANUS reactor of the Argonne National Laboratory, in *Radiobiological Applications of Neutron Irradiation*, International Atomic Energy Agency, Vienna, pp. 211-228.
- Grahn, D., C. Fox, B.J. Wright, and B.A. Carnes, 1994, *Studies of Acute and Chronic Radiation Injury at the Biological and Medical Research Division, Argonne National Laboratory, 1953-1970: Description of Individual Studies, Data Files, Codes, and Summaries of Significant Findings*, Argonne National Laboratory report ANL-94/26, 99 pp.
- Grahn, D., L.S. Lombard, and B.A. Carnes, 1992, The comparative tumorigenic effects of fission neutrons and cobalt-60  $\gamma$  rays in the B6CF<sub>1</sub> mouse, *Radiation Research* 129:19-36.

- Grahn, D., J.F. Thomson, B.A. Carnes, F.S. Williamson, and L.S. Lombard, 1986, Comparative biological effects of low dose, low dose-rate exposures to fission neutrons from the JANUS reactor or to Co-60 gamma rays, *Nuclear Science Applications* 2:385-396.
- Grdina, D.J., B.A. Carnes, D. Grahn, and C.P. Sigdestad, 1991a, Protection against late effects of radiation by S-2-(3-aminopropylamino)-ethylphosphorothioic acid, *Cancer Research* 51:4125-4130.
- Grdina, D.J., B.J. Wright, and B.A. Carnes, 1991b, Protection by WR-151327 against late-effect damage from fission-spectrum neutrons, *Radiation Research* 128:S124-S127.
- ICRU, 1979, *Quantitative Concepts and Dosimetry in Radiobiology*, Report 30, International Commission on Radiation Units and Measurements, Bethesda, Maryland, pp. 44-47.
- Marshall, I.R., and F.S. Williamson, 1985, Microdosimetric spectra measurements of JANUS neutrons, *Radiation Protection Dosimetry* 13:111-115.
- Neary, G.J., R.J. Munson, and R.H. Mole, 1957, *Chronic Radiation Hazards*, Pergamon Press, New York, pp. 190.
- Neary, G.J., and F.S. Williamson, 1961, A simple method of fast-neutron dosimetry for use in radiobiology and an intercomparison with some methods used in the United States, in *Selected Topics in Radiation Dosimetry*, International Atomic Energy Agency, Vienna, pp. 463-471.
- Sacher, G.A., and R.W. Hart, 1978, Longevity, aging, and comparative cellular and molecular biology of the house mouse, *Mus musculus*, and the white-footed mouse, *Peromyscus leucopus*, *Birth Defects* 14:76-96.
- Thomson, J.F., and D. Grahn, 1988, Life shortening in mice exposed to fission neutrons and  $\gamma$  rays. VII. Effects of 60 once-weekly exposures, *Radiation Research* 115:347-360.
- Thomson, J.F., and D. Grahn, 1989, Life shortening in mice exposed to fission neutrons and  $\gamma$  rays. VIII. Exposures to continuous  $\gamma$  radiation, *Radiation Research* 118:151-160.
- Thomson, J.F., F.S. Williamson, and D. Grahn, 1983, Life shortening in mice exposed to fission neutrons and  $\gamma$  rays. III. Neutron exposures of 5 and 10 rad, *Radiation Research* 93:205-209.
- Thomson, J.F., F.S. Williamson, and D. Grahn, 1985a, Life shortening in mice exposed to fission neutrons and  $\gamma$  rays. IV. Further studies with fractionated neutron exposures, *Radiation Research* 103:77-88.
- Thomson, J.F., F.S. Williamson, and D. Grahn, 1985b, Life shortening in mice exposed to fission neutrons and  $\gamma$  rays. V. Further studies with low single doses, *Radiation Research* 104:420-428.

- Thomson, J.F., F.S. Williamson, and D. Grahn, 1986, Life shortening in mice exposed to fission neutrons and  $\gamma$  rays. VI. Studies with the white-footed mouse, *Peromyscus leucopus*, *Radiation Research* 108:176-188.
- Thomson, J.F., F.S. Williamson, D. Grahn, and E.J. Ainsworth, 1981a, Life shortening in mice exposed to fission neutrons and  $\gamma$  rays. I. Single and short-term fractionated exposures, *Radiation Research* 86:559-572.
- Thomson, J.F., F.S. Williamson, D. Grahn, and E.J. Ainsworth, 1981b, Life shortening in mice exposed to fission neutrons and  $\gamma$  rays. II. Duration-of-life and long-term fractionated exposures, *Radiation Research* 86:573-579.
- Vogel, H.H. Jr., R.A. Blomgren, and N.J.G. Bohlin, 1953, Gamma-neutron radiation chamber for radiobiological studies, *Nucleonics* 11:28-31.
- Williamson, F.S., and N.A. Frigerio, 1972, Field mapping and depth dosimetry in the JANUS high flux irradiation room—a fast neutron facility for biological research, in *Proceedings of the First Symposium on Neutron Dosimetry in Biology and Medicine*, vol. II, Commission of the European Communities, Luxembourg, pp. 743-755.
- Williamson, F.S., N.A. Frigerio, G.L. Holmblad, J.E. Trier, and E.G. Johnson Jr., 1971, Neutron and gamma dosimetry for the JANUS program, in *Biological and Medical Research Division Annual Report*, Argonne National Laboratory report ANL-7870, pp. 5-8.
- Williamson, F.S., N.A. Frigerio, G.L. Holmblad, J.E. Trier, and E.G. Johnson Jr., 1972, Neutron dosimetry for the JANUS program, in *Biological and Medical Research Division Annual Report*, Argonne National Laboratory report ANL-7970, pp. 9-11.
- Williamson, F.S., G.L. Holmblad, J.E. Trier, and E.G. Johnson Jr., 1973, Dosimetry of cobalt-60 gamma radiation in the JM-2 experiment, in *Biological and Medical Research Division Annual Report*, Argonne National Laboratory report ANL-8070, pp. 26-27.

**TABLE 1 Composition of Combined Pathology Database <E>**

Group	Included Pathology
1	Cause of death undetermined
<u>Tumor pathology</u>	
2	Lymphoreticular tumors
3	Vascular tumors
4	Connective tissue tumors other than lymphoreticular and vascular
5 <sup>a</sup>	Respiratory system
6 <sup>a</sup>	Harderian gland
7 <sup>a</sup>	Liver and gallbladder
8 <sup>a</sup>	Kidneys and urinary bladder
9 <sup>a</sup>	Gastrointestinal tract
10 <sup>a</sup>	Adrenal gland
11 <sup>a</sup>	Pituitary gland
12 <sup>a</sup>	Thyroid gland
13 <sup>a</sup>	Testes and seminal vesicles
14 <sup>a</sup>	Mammary glands
15 <sup>a</sup>	Uterus
16 <sup>a</sup>	Ovaries
17 <sup>a</sup>	Skin and other epithelial tissue tumors not included in groups 5 through 16
18	Any secondary connective tissue tumor at any site
19	Secondary tumors of Harderian gland origin, any site
20	Secondary tumors of respiratory system origin, any site
21	All other secondary tumors, any site
<u>Nontumor pathology</u>	
22	Acute or chronic disease of the liver
23	Acute or chronic pulmonary disease
24	Acute or chronic cardiovascular disease
25	Acute or chronic renal disease
26	Ovarian cyst
27	Amyloid infiltration
28	All other nonneoplastic diseases, acute or chronic

<sup>a</sup> Groups 5 through 17 involve neoplastic diseases of epithelial tissue origin, with the exception of certain tumors of mixed origin involving the adrenal and mammary glands.

**TABLE 2 Composition of Combined Pathology Database <F>**

Group	Included Pathology
1	Any primary tumor of connective and/or epithelial tissue origin, including ovarian tumors
2	Any primary connective tissue tumor
3	Any primary epithelial tissue tumor, excluding ovarian tumors
4	Lymphoreticular tumors (group 2, database <E>)
5 <sup>a</sup>	Histiocytic lymphoma, type A reticulum cell tumor
6 <sup>a</sup>	Lymphocytic-lymphoblastic leukemia
7 <sup>a</sup>	Lymphocytic-lymphoblastic lymphoma
8 <sup>a</sup>	Unclassified lymphoma
9 <sup>a</sup>	Mixed histiocytic-lymphocytic lymphoma, type B reticulum cell tumor
10 <sup>a</sup>	All other lymphoreticular tumors
11 <sup>b</sup>	Hemangioma, any site
12 <sup>b</sup>	Angiosarcoma, any site
13	All vascular tumors (group 3, database <E>)
14	Fibroma, fibrosarcoma, undifferentiated sarcoma, any site
15	All other connective tissue tumors not included in groups 5 through 14
16	Connective tissue tumors other than lymphoreticular and vascular (group 4, database <E>)
17	Liver, hepatocellular tumors
18	Liver, bile duct tumors
19	Adrenal cortical tumors
20	Adrenal medullary tumors
21	Ovary, all tumors (group 16, database <E>)
22 <sup>c</sup>	Ovary, granulosa cell tumor
23 <sup>c</sup>	Ovary, tubular adenoma
24 <sup>c</sup>	Ovary, luteoma (thecoma)
25 <sup>c</sup>	All other ovarian tumors
26	Tumors of the kidneys, liver, gastrointestinal system, and skin
27	Tumors of the mammary glands, adrenal glands, pituitary gland, thyroid gland, uterus, testes, and seminal vesicles
28	As in group 27 plus the Harderian gland

<sup>a</sup> Specific cellular subclasses of the lymphoreticular tumors.

<sup>b</sup> Subclasses of vascular tumors.

<sup>c</sup> Subclasses of ovarian tumors.

**TABLE 3 Composition of Combined Pathology Database <H>**

Group	Included Pathology
1	Any primary tumor of connective and/or epithelial tissue origin, including ovarian tumors (group 1, database <F>)
2	Any primary connective tissue tumor (group 2, database <F>)
3	Any primary epithelial tissue tumor excluding ovarian tumors (group 3, database <F>)
4	Lymphoreticular tumors (group 2, database <E>)
5	Lymphosarcoma
6	Reticulum cell sarcoma
7	Lymphocytic leukemia
8	All carcinomas
9	All sarcomas
10	All fibromas
11	All fibrosarcomas
12	Alveologenic tumor (adenoma), benign
13	Alveologenic tumor (adenocarcinoma), malignant
14	All adrenal tumors (group 10, database <E>)
15	Adrenal cortical tumors (group 19, database <F>)
16	Adrenal medullary tumors (group 20, database <F>)
17	Hepatocellular tumors (group 17, database <F>)
18	Kidney tumors
19	All mammary gland tumors (group 14, database <E>)
20	All gastrointestinal tract tumors (group 9, database <E>)
21	All bone tumors
22	Metastasis from lung tumor to any site (group 20, database <E>)
23	Metastasis from kidney to any site
24	Metastasis from Harderian gland tumor to any site (group 19, database <E>)
25	Metastasis from bone tumor to any site
26	Metastasis from any site to lung
27	Metastasis from any site to kidney
28	All metastatic tumors (secondaries)

**TABLE 4 JANUS Program Records Summary**

Experiment No. (JM-)	Input	Death Records	Gross Pathology	Histopathology
2	11,590	9,947	9,205	7,838
3	3,280	2,867	2,732	2,204
4K	6,070	4,739	4,465	3,193
4W	2,200	1,519	1,462	0
4L1	620	598	567	364
4L2	525	516	508	371
7	2,735	2,676	2,554	438
8	1,880	1,292	1,197	239
9	5,450	5,385	4,923	1,465
10	2,390	2,187	1,959	0
12	600	600	537	0
13	7,895	6,317	5,935	2,760
14	4,000	3,978	3,668	623
Total	49,235	42,621	39,712	19,495

**TABLE 5 Analysis of Concordance between Gross and Microscopic Findings for the Classifications of Lethal (L), Lethal Plus Contributory (LC), and All Observed (LCN) Pathology (percentage of gross diagnoses confirmed by histopathology and number of confirmed events [n])**

Tumor Type or Grouping	L		LC		LCN	
	(%)	n	(%)	n	(%)	n
All primary tumors	<u>94.1</u>	8,828	<u>97.8</u>	9,177	<u>98.6</u>	12,222
All connective tissue	<u>93.2</u>	5,540	<u>96.6</u>	5,740	<u>95.2</u>	7,346
Lymphoreticular	<u>96.7</u>	4,432	<u>98.0</u>	4,494	<u>96.0</u>	5,501
Vascular	<u>72.7</u>	497	<u>89.5</u>	612	<u>88.5</u>	1,015
Other connective tissue tumors	52.4	354	58.9	398	47.7	605
All epithelial tissue	76.0	2,394	<u>88.9</u>	2,800	<u>89.2</u>	7,456
Lung	<u>86.9</u>	1,643	<u>98.0</u>	1,853	<u>91.7</u>	5,489
Liver	52.6	170	71.5	231	60.0	689
Harderian gland	78.5	142	<u>87.3</u>	158	81.2	1,333
Ovary	23.4	68	33.8	98	68.3	1,281
Kidneys, liver, gastrointestinal, and skin	53.5	416	69.4	540	67.5	1,681
Endocrine and reproductive system	53.3	256	69.0	331	70.6	1,934

TABLE 6 Analysis of Discordance between Gross and Microscopic Pathology<sup>a</sup>

Diagnostic Code, n, Discordance (%)	Connective Tissue				Epithelial Tissue		
	CDU	LR	VAS	CON	ADN	LIV	OVE
CDU, n = 1,530 63.1	966 100.0	530 54.9	68 7.0	33 3.4	81 8.4	14 1.4	8 0.8
LR, n = 4,585 3.3	67 43.8	153 100.0	25 16.3	4 2.6	22 14.4	0 0.0	2 1.3
VAS, n = 684 27.3	65 34.8	61 32.6	187 100.0	3 1.6	13 7.0	9 4.8	0 0.0
CON, n = 676 47.6	59 18.3	54 16.8	108 33.5	322 100.0	24 7.5	2 0.6	0 0.0
ADN, n = 1,890 13.1	42 17.0	138 55.9	13 5.3	9 3.6	247 100.0	1 0.4	1 0.4
LIV, n = 323 47.4	21 13.7	60 39.2	37 24.2	3 2.0	14 9.2	153 100.0	0 0.0
OVE, n = 290 76.6	58 26.1	52 23.4	41 18.5	2 0.9	6 2.7	5 2.3	222 100.0

<sup>a</sup> Values on the diagonal (boxed) are the number of discordant events in the diagnostic class stated as 100%. The other values in each row give the number of diagnoses reclassified to another diagnostic code (column) and the percentage of the discordants so reclassified.

Diagnostic codes are as follows:

CDU = Cause of death undetermined

LR = Lymphoreticular tumor

VAS = Vascular tumor

CON = Other connective tissue tumors (fibroma, sarcoma)

ADN = Lung tumor

LIV = Liver tumor (hepatocellular)

OVE = Ovarian tumor

TABLE 7 Inventory of Death and Pathology Records for Experiment JM-2

Radiation Quality	Total Dose (cGy)	Treatment Code <sup>a</sup>	Males					Females				
			Input	Death Records	MAS <sup>b</sup> ± SE (d)	MACRO Records	MICRO Records	Input	Death Records	MAS <sup>b</sup> ± SE (d)	MACRO Records	MICRO Records
Control	0	AC	200	159	835 ± 15	156	123	200	145	863 ± 15	140	124
		DC	200	158	859 ± 14	49	32	200	194	818 ± 15	64	51
		EC	200	169	864 ± 15	168	137	200	194	832 ± 13	186	165
		HC	200	157	840 ± 18	68	44	200	120	816 ± 18	38	27
		SO	200	200	843 ± 13	198	174	200	200	852 ± 13	198	185
γ Rays	855	AI	200	148	711 ± 15	146	113	200	93	690 ± 19	87	78
		BI	200	156	691 ± 14	154	132	200	124	673 ± 16	122	112
		EI	200	151	697 ± 14	149	113	200	121	687 ± 14	117	105
		HI	200	152	666 ± 14	150	122	200	125	641 ± 14	119	105
		DI	200	148	619 ± 14	146	115	200	200	610 ± 11	193	166
		S1	400	386	810 ± 10	382	328	400	397	790 ± 9	391	367
		S2	200	185	727 ± 13	179	155	200	198	706 ± 12	193	183
		S3	200	196	460 ± 17	184	133	200	200	431 ± 17	182	136
		Y2 <sup>c</sup>	200	200	710 ± 13	192	157	200	99	693 ± 18	95	87
		Y3 <sup>c</sup>	200	200	492 ± 15	180	146	200	100	486 ± 18	94	72
		Z2 <sup>d</sup>	200	193	635 ± 14	189	160	200	100	601 ± 18	94	81
		Z3 <sup>d</sup>	200	198	520 ± 13	181	147	200	95	498 ± 18	92	71
Neutrons	240	AI	200	151	546 ± 16	148	118	200	108	505 ± 15	99	81
		BI	200	134	518 ± 14	130	101	200	121	499 ± 13	111	97
		EI	200	149	544 ± 14	147	119	200	128	495 ± 12	118	100
		HI	200	149	572 ± 14	144	124	200	136	528 ± 12	131	110
		DI	200	149	666 ± 15	146	115	200	167	675 ± 13	163	147
		S1	400	383	789 ± 10	382	335	400	380	759 ± 10	366	343
		S2	200	178	724 ± 14	175	157	200	200	667 ± 14	185	173
		S3	200	157	632 ± 15	154	135	200	199	580 ± 13	187	167
		Y2 <sup>c</sup>	200	200	693 ± 15	197	169	200	100	655 ± 18	93	83
		Y3 <sup>c</sup>	200	199	612 ± 13	184	161	200	99	593 ± 15	96	84
		Z2 <sup>d</sup>	200	199	609 ± 12	193	159	200	95	600 ± 18	91	76
		Z3 <sup>d</sup>	200	200	570 ± 13	193	153	200	100	573 ± 16	96	85

<sup>a</sup> See Appendix J for details.<sup>b</sup> Mean after-survival [MAS] values based on all death records.<sup>c</sup> 194 days of age at exposure.<sup>d</sup> 287 days of age at exposure.

TABLE 8 Inventory of Death and Pathology Records for Experiment JM-3

Radiation Quality	Total Dose (cGy)	Treatment Code <sup>a</sup>	Males				Females					
			Input	Death Records	MAS <sup>b</sup> ± SE (d)	MACRO Records	MICRO Records	Input	Death Records	MAS <sup>b</sup> ± SE (d)	MACRO Records	MICRO Records
Control	0	S0	200	200	872 ± 13	191	142	200	190	820 ± 16	175	152
γ Rays	90	S4	200	199	858 ± 14	189	138	200	200	825 ± 13	189	171
	143	S6	160	160	827 ± 16	150	113	80	7	- <sup>c</sup>	7	6
	206	S6	160	160	802 ± 16	155	122	80	6	- <sup>c</sup>	6	4
	417	S7	120	120	744 ± 18	117	102	60	60	706 ± 27	54	49
Neutrons	569	S8	120	120	646 ± 20	118	99	120	78	645 ± 25	74	66
	20	S4	250	249	826 ± 13	242	189	250	244	778 ± 13	231	208
	40	S6	200	199	798 ± 14	181	153	80	7	- <sup>c</sup>	6	5
	60	S6	200	200	780 ± 14	191	169	80	7	- <sup>c</sup>	7	7
	120	S7	120	120	719 ± 18	117	104	60	7	- <sup>c</sup>	7	5
	160	S8	120	119	714 ± 18	115	101	120	120	646 ± 17	117	99
	240	SL	50	50	678 ± 25	49	0	0	0	0	0	0
	240	SH	60	45	702 ± 25	44	0	0	0	0	0	0

<sup>a</sup> See Appendix J for details.

<sup>b</sup> MAS values based on all death records.

<sup>c</sup> Females discarded before about 500 d after exposure.

TABLE 9 Inventory of Death and Pathology Records for Experiments JM-4K and JM-4W

Radiation Quality	Total Dose (cGy)	Treatment Code	Males					Females				
			Input	Death Records	MAS <sup>b</sup> ± SE (d)	MACRO Records	MICRO Records	Input	Death Records	MAS <sup>b</sup> ± SE (d)	MACRO Records	MICRO Records
<b>JM-4K:</b>												
Control	0	K0	280	195	928 ± 15	185	129	180	140	890 ± 16	134	110
γ Rays	206	K1	675	598	854 ± 8	585	391	120	7	- <sup>c</sup>	7	0
	417	K2	455	400	802 ± 9	385	278	400	394	783 ± 9	378	329
	959	K3	275	194	725 ± 12	185	146	80	5	-	5	0
	1919	K4	225	150	441 ± 12	143	105	60	13	-	12	0
	3820	K5	190	147	269 ± 7	117	48	30	25	244 ± 12	23	0
	5111	K6	140	100	143 ± 3	50	0	40	40	112 ± 2	28	0
<b>Neutrons</b>												
	20	K1	675	593	846 ± 8	563	328	600	593	800 ± 8	578	496
	40	K2	475	400	799 ± 10	378	259	80	3	-	3	0
	60	K3	275	194	762 ± 15	184	139	40	0	-	0	0
	120	K4	225	150	666 ± 16	145	121	30	0	-	0	0
	168	K5	190	150	631 ± 15	141	110	150	150	596 ± 13	144	127
	320	K6	140	95	511 ± 16	90	77	20	3	-	2	0
<b>JM-4W:</b>												
Control	0	W0	0	0				400	324	853 ± 11	314	0
γ Rays	807	W1	0	0				450	307	703 ± 9	302	0
	2690	W2	0	0				500	333	351 ± 7	304	0
<b>Neutrons</b>												
	80	W1	0	0				400	263	695 ± 10	261	0
	240	W2	0	0				450	292	554 ± 10	281	0

<sup>a</sup> See Appendix J for details.

<sup>b</sup> MAS values based on all death records.

<sup>c</sup> Dash indicates a number of deaths too small to allow estimation of MAS.

**TABLE 10 Inventory of Death and Pathology Records for Experiments JM-4L1 and JM-4L2 (only males used)**

Radiation Quality	Total Dose (cGy)	Treatment Code <sup>a</sup>	Input	Death Records	MAS <sup>b</sup> ± SE (d)	MACRO Records	MICRO Records
<b>JM-4L1:</b>							
Control	0	L0	200	189	862 ± 15	181	111
γ Rays	206	L1	200	194	830 ± 13	180	118
	417	L2	100	99	806 ± 22	97	57
	959	L3	80	76	675 ± 23	72	48
	1918	L4	40	40	579 ± 32	37	30
<b>JM-4L2:</b>							
Control	0	LC	175	173	803 ± 16	172	120
γ Rays	529	L5	175	170	767 ± 15	165	121
	1070	L6	100	99	719 ± 16	99	79
	2460	L7	75	74	608 ± 22	72	51

<sup>a</sup> See Appendix J for details.

<sup>b</sup> MAS values based on all death records.

TABLE 11 Inventory of Death and Pathology Records for Experiment JM-7

Radiation Quality	Total Dose (cGy)	Treatment Code <sup>a</sup>	Males				Females					
			Input	Death Records	MAS <sup>b</sup> ± SE (d)	MACRO Records	MICRO Records	Input	Death Records	MAS <sup>b</sup> ± SE (d)	MACRO Records	MICRO Records
Control	0	00	330	310	887 ± 11	293	0	180	175	886 ± 15	164	0
γ Rays	417	Q1	135	135	862 ± 16	131	92	30	27	786 ± 41	25	0
	1918	Q2	180	178	627 ± 12	167	124	180	178	621 ± 10	166	0
Neutrons	40	Q1	150	146	789 ± 15	138	95	30	30	763 ± 38	29	0
	160	Q2	200	189	632 ± 12	180	127	200	194	599 ± 11	187	0
γ Rays	206	R1 <sup>c</sup>	150	148	460 ± 14	147	0	50	50	408 ± 24	47	0
	569	R2 <sup>c</sup>	180	178	392 ± 11	168	0	180	176	374 ± 12	175	0
Neutrons	40	R1 <sup>c</sup>	150	150	429 ± 13	147	0	50	49	434 ± 23	46	0
	160	R2 <sup>c</sup>	180	172	410 ± 11	174	0	180	177	395 ± 12	170	0

<sup>a</sup> See Appendix J for details.

<sup>b</sup> MAS values based on all death records.

<sup>c</sup> 515 d of age at exposure to the single dose indicated.

TABLE 12 Inventory of Death and Pathology Records for Experiment JM-8

Radiation Quality	Dose per Week (cGy)	Treatment Code <sup>a</sup>	Males					Females				
			Input	Death Records	MAS <sup>b</sup> ± SE (d)	MACRO Records	MICRO Records	Input	Death Records	MAS <sup>b</sup> ± SE (d)	MACRO Records	MICRO Records
Control	0	U0	140	60	904 ± 25	54	40	50	50	853 ± 22	44	39
γ Rays	6.95	U1	260	181	819 ± 13	170	56	180	174	819 ± 13	158	0
	17.4	U2	200	120	755 ± 15	115	43	20	20	670 ± 35	15	0
	31.9	U3	170	86	631 ± 14	79	0	15	15	603 ± 37	13	0
Neutrons	0.67	U1	260	179	783 ± 14	169	61	180	169	737 ± 13	158	0
	1.67	U2	200	112	680 ± 13	105	0	20	20	608 ± 36	19	0
	2.67	U3	170	91	644 ± 17	85	0	15	15	553 ± 32	13	0

<sup>a</sup> See Appendix J for details.

<sup>b</sup> MAS values based on all death records.

TABLE 13 Inventory of Death and Pathology Records for Experiment JM-9

Radiation Quality	Total Dose (cGy)	Treatment Code <sup>a</sup>	Males				Females					
			Input	Death Records	MAS <sup>b</sup> ± SE (d)	MACRO Records	MICRO Records	Input	Death Records	MAS <sup>b</sup> ± SE (d)	MACRO Records	MICRO Records
Preliminary study:												
Control	0	X0 XX	200 0	200	935 ± 13	189	0	200 200	199 200	891 ± 14 866 ± 13	184 186	0 0
Neutrons	5 10	X2 X3	0 200	200	876 ± 14	193	0	300 200	289 200	850 ± 12 827 ± 13	261 186	0 0
	10	XX	0	0			0	200	197	846 ± 15	183	0
Final study:												
Control	0	XC	0	0			0	750	739	856 ± 7	656	248
γ Rays	22.5 45 90	X1 X2 X3	0 0 0	0			0	500 350 200	497 346 194	844 ± 9 850 ± 11 819 ± 14	453 314 177	177 121 73
Neutrons	1 2.5 5 10 20 40	X4 X5 X6 X7 X8 X9	0 0 0 0 0 0	0			0	750 450 350 250 200 150	735 445 349 245 200 150	859 ± 7 848 ± 9 822 ± 11 805 ± 13 797 ± 13 753 ± 16	661 411 312 230 183 142	253 169 132 91 78 123

<sup>a</sup> See Appendix J for details.<sup>b</sup> MAS values based on all death records.

**TABLE 14 Inventory of Death and Pathology Records for Experiment JM-10 (males only)**

Radiation Quality	Total Dose (cGy)	Treatment Code <sup>a</sup>	Input	Death Records	MAS <sup>b</sup> ± SE (d)	MACRO Records	MICRO Records
Control	0	V0	245	211	1255 ± 35	181	0
	0	W0	210	203	1321 ± 33	171	0
γ Rays	90	V1	200	189	1225 ± 38	164	0
	143	V2	200	182	1211 ± 36	158	0
	206	V3	200	190	1185 ± 35	175	0
	417	V4	170	159	1027 ± 35	146	0
Neutrons	20	V1	200	182	1183 ± 34	161	0
	40	V2	200	180	1179 ± 30	167	0
	80	V3	150	141	979 ± 31	121	0
	160	V4	150	140	890 ± 25	129	0
	40	VV	250	219	1151 ± 29	203	0
	160	VW	215	191	841 ± 22	183	0

<sup>a</sup> See Appendix J for details.

<sup>b</sup> MAS values based on all death records.

**TABLE 15 Inventory of Death and Pathology Records for Experiment JM-12**

Radiation Quality	Total Dose (cGy)	Treatment Code <sup>a</sup>	Input	Death Records	MAS <sup>b</sup> ± SE (d)	MACRO Records	MICRO Records
Control	0	J0	120	120	904 ± 19	112	0
Neutrons	240	J1	120	120	668 ± 18	98	0
	240	J2	120	120	620 ± 21	112	0
	240	J4	120	120	548 ± 22	105	0
	240	J6	120	120	601 ± 19	110	0

<sup>a</sup> See Appendix J for details.

<sup>b</sup> MAS values based on all death records.

TABLE 16 Inventory of Death and Pathology Records for Experiment JM-13

Radiation Quality	Total Dose (cGy)	Treatment Code <sup>a</sup>	Males					Females				
			Input	Death Records	MAS <sup>b</sup> ± SE (d)	MACRO Records	MICRO Records	Input	Death Records	MAS <sup>b</sup> ± SE (d)	MACRO Records	MICRO Records
Control	0	0X	810	592	882 ± 8	565	196	600	584	873 ± 8	541	214
γ Rays	100	1X	600	594	861 ± 7	571	212	600	598	846 ± 8	552	223
	200	2X	220	178	840 ± 14	168	115	180	174	819 ± 15	167	127
	300	3X	295	83	832 ± 20	79	57	80	79	782 ± 20	76	59
	450	4X	290	86	813 ± 19	83	62	80	75	784 ± 18	70	57
	600	5X	290	90	793 ± 20	85	56	80	79	745 ± 19	74	59
Neutrons	2	1X	600	566	893 ± 8	538	174	600	568	869 ± 8	528	218
	7.5	2X	455	271	869 ± 11	255	94	250	247	837 ± 12	215	95
	13.5	3X	250	242	855 ± 11	230	78	250	237	809 ± 11	221	104
	21	4X	450	254	817 ± 12	231	94	250	244	790 ± 12	230	111
	30	5X	150	149	779 ± 16	141	102	150	150	771 ± 15	142	121
	40	6X	285	98	805 ± 18	95	67	80	79	717 ± 19	78	65

<sup>a</sup> See Appendix J for details.<sup>b</sup> MAS values based on all death records.

TABLE 17 Inventory of Death and Pathology Records for Experiment JM-14

Radiation Quality	Total Dose (cGy)	Treatment Code <sup>a</sup>	Males				Females					
			Input	Death Records	MAS <sup>b</sup> ± SE (d)	MACRO Records	MICRO Records	Input	Death Records	MAS <sup>b</sup> ± SE (d)	MACRO Records	MICRO Records
Control	0	0P <sup>c</sup>	200	194	886 ± 13	173	0	200	199	858 ± 13	182	0
		0S <sup>d</sup>	200	199	891 ± 13	189	0	200	200	858 ± 14	188	0
γ Rays	206	C0 <sup>e</sup>	200	199	790 ± 14	184	0	200	198	770 ± 13	186	157
		CP	200	198	821 ± 14	182	0	200	200	824 ± 13	180	161
		DP	200	199	796 ± 15	182	0	200	200	738 ± 13	192	0
Neutrons	10	A0	200	198	850 ± 13	180	0	200	199	812 ± 14	182	156
		AP	200	199	843 ± 16	183	0	200	199	836 ± 14	186	149
		AR <sup>f</sup>	200	200	874 ± 14	186	0	200	200	836 ± 13	184	0
		BP	200	199	797 ± 14	183	0	200	200	762 ± 13	186	0
		BR	200	200	797 ± 14	182	0	200	198	751 ± 13	178	0

<sup>a</sup> See Appendix J for details.

<sup>b</sup> MAS values based on all death records.

<sup>c</sup> Code P: treated with radioprotector WR-2721.

<sup>d</sup> Code S: treated with saline.

<sup>e</sup> Code 0: no treatment.

<sup>f</sup> Code R: treated with radioprotector WR-151327.